CHAPTER V
RESULTS AND DISCUSSION

Results from investigation of the synthesized catalyst properties will be interpreted in this chapter. Some physical properties, chemical properties and catalytic behavior of synthesized Co-TS-1 catalysts, including effects of the amount of cobalt in the samples are revealed by the characterization methods and the reaction test.

In this chapter, results and discussion are divided into two parts. The first one is the results of characterization of Co-TS-1 samples using different analytical techniques, such as XRF, SEM, XRD, BET, FT-IR and NH_3-TPD. The second part is the results of catalytic activity study of 2-propanol oxidation reactions.

5.1 Catalyst characterization of Co-TS-1 samples

5.1.1 Determination of Chemical compositions of the synthesized Co-TS-1 Samples

The chemical composition of the synthesized catalysts was determined by x-ray fluorescence spectroscopy (XRF). The results from raw data of XRF can be calculated by using two methods. The first method is calculated by base on standard solution that is shown in Table 5.1. Another is calculated from information library in software of XRF instrument that shown in Appendix C.

Table 5.1 Chemical composition of the synthesized Co-TS-1 samples.

Sample	Types of Salts	Loading Solution	Chemical composition by mole				
			Si (%)	Ti (%)	Co (%)	Si/Ti	Si/Co
batch 1	$Co(NO_3)_2 \cdot 6H_2O$	A1	32.92	0.24	0.26	137.26	127.38
batch 2		A2	33.00	0.33	0	100.93	∞
batch 3		C1	33.01	0.21	0.16	154.13	204.78
batch 4		A1andA2	32.99	0.27	0.11	123.56	292.45
batch 5	$CoCl_2 \cdot 6H_2O$	A1	32.84	0.31	0.26	106.56	124.41
batch 6		C1	32.74	0.31	0.42	105.93	77.69
batch 7		A1andA2	32.92	0.32	0.13	102.04	260.63
Batch 8	$Co(C_2H_3O_2)_2 \cdot 4H_2O$	A1	32.78	0.29	0.40	114.57	82.60
Batch 9		C1	32.70	0.33	0.44	98.48	73.78
batch 10		A1andA2	32.92	0.28	0.20	117.56	167.65

In Table 5.1, the quantitative determination of Co, Ti, Si contents and the ratios of Si/Ti and Si/Co in the Co-TS-1 catalysts are given. The result of Co-TS-1 batch 2 that adding the cobalt salts in only the decant solution (solution A2) results in the loss of cobalt. This is because the added cobalt exists in the discarded gel of the decant solution. Very small amount of cobalt ion remain in the decant solution. When this decant solution is used to prepare the catalyst in the final step, it contributes no cobalt to the formed catalysts. As can be seen from Table 5.1, putting cobalt nitrate salt in the A2 solution only results in Ti and Si contained in the synthesized samples but no cobalt in the obtained catalysts. Similarly, loading cobalt in both gel and decantation solutions (A1 and A2), batch 4, 7, 10, shows the less amount of cobalt than loading cobalt salt in either at the same desired ratio. Therefore, dividing the added cobalt salts between A1 and A2 solution results in lossing half of the cobalt can be incorporated in the obtained catalyst.

As can be seen, the ratios by mole of Si/Ti and Si/Co are different from the desired ratio value (as shown in Chapter III). It may come from many reasons such as the different conditions that we used. Variation in some synthesis parameters was found to have a significant influence upon the extent of titanium and cobalt incorporation. One of the reasons causing that problem may be the reaction time in the autoclave during synthesizing. The reaction time used in our experiment may not long enough for titanium and cobalt forming into framework in a large amount.

Another point from this section, about the comparative types of cobalt salt (nitrate, chloride, acetate), the anions of cobalt salt have influenced on the amount of cobalt that incorporate into the synthesized catalyst. In order to explain the effect of cobalt precursors on the amount of cobalt can be incorporated into the obtained catalysts, it is worth to mention the behavior of Co cation in the solutions. Any dissolvable Co^{2+} salts, when dissolve in water, the simplest ion forms is the pink hexaaquacobalt (II) ion ($(Co(H_2O)_6)^{2+}$).

In the presence of OH^- ion, the hydroxide ions remove hydrogen ions from the water ligands attached to the cobalt ion according to the following equation.

$$(Co(H_2O)_6)^{2+} + 2\ OH^- \rightarrow (Co(H_2O)_4(OH)_2) + 2H_2O \qquad (5.1)$$

The formed $(Co(H_2O)_4(OH)_2)$ is insoluble in water and a precipitated of $(Co(H_2O)_4(OH)_2)$ is formed.

In an acidic solution with the presence of Cl^- ion, the six water molecules in the ligand $(Co(H_2O)_6)^{2+}$ are replaced by four Cl^- ions according to the following equation.

$$(Co(H_2O)_6)^{2+} + 4Cl^- \underset{\text{basic}}{\overset{\text{acidic}}{\rightleftharpoons}} (CoCl_4)^{2-} + 6H_2O \qquad (5.2)$$

The reaction above is reversible.

Since Co^{2+} is weak Lewis acid, the solution of a cobalt salt will become slightly acidic. The acidity of the solution will depend on the role of the anion of the salt. Cl^- and NO^{3-} ions are conjugate bases of strong acid (HCl and HNO_3, respectively), therefore, these two ions prefer to stay in their original form and play no role on manipulating the pH of the solutions. On the contrary, CH_3COO^- is a

conjugate base of a weak acid (CH_3COOH), this ion can neutralize some acid species present in the solution. Therefore, the solution of the acetate salt ($Co(C_2H_3O_2)_2 \cdot 4H_2O$) has higher pH value than the solution of the chloride ($CoCl_2 \cdot 6H_2O$) and the nitrate ($Co(NO_3)_2 \cdot 6H_2O$) salts. The consequence is the preparation using ($Co(C_2H_3O_2)_2 \cdot 4H_2O$) salt requires less amount of NaOH solution (or do not need) to adjust the pH of the C1 solution to be in the range 9-11

In the gel preparation step, three solutions (A1-acidic, B1-basic, C1-basic) have to be mixed altogether. For the preparation using cobalt nitrate, if the cobalt salt is dissolved in the C1 solution, part of Co^{2+} may form the precipitate ($Co(H_2O)_4(OH)_2$) before the gel is formed. The precipitate formed was washed out during the washing step as can be seen from color of the washed water. Dissolving nitrate salt in the A1 solution, leaves the Co^{2+} ion in its ligand form. Gradually, dropping the A1 solution into the C1 solution gives more chance for the Co^{2+} ligand to incorporate into the forming gel. Therefore, putting nitrate salt in the A1 solution yield higher amount of cobalt in the obtained catalysts than putting nitrate salts in the C1 solution.

The behavior of $CoCl_2$ is slightly different from the behavior of $(CoNO_3)_2$, especially when dissolving the salt in the C1 solution. Dissolving the nitrate salt, all the cobalt cations will form $(Co(H_2O)_6)^{2+}$ which further reacts with OH^- in the solution. This results in the lower of the pH value of the C1 solution. For the chloride salt, part of the cobalt cations exist in the form $(CoCl_4)^{2-}$ which does not react with OH^- in the C1 solution. Thus, the pH value of the C1 solution with the chloride salt is higher than the pH value of the C1 solution of the nitrate salt. For this reason, the both amount of NaOH solution to adjust the pH and a precipitated of ($Co(H_2O)_4(OH)_2$) of chloride salt are less than nitrate salt. As forming gel, the C1 solution of chloride salt is adjusted pH value with A1 and B1 solutions to be a basic in range 9-11, therefore, the reverse of equation 5.2 has occurred. The formed $(CoCl_4)^{2-}$ is changed to $(Co(H_2O)_6)^{2+}$ in order to prepare Co^{2+} to form the gel. Therefore, adding chloride salt in C1 solution yield higher amount of cobalt in the obtained catalysts than putting chloride salt in A1 solution.

The acetate salt of cobalt behaves differently from the chloride and nitrate salts. Putting the acetate salt in the C1 solution does not lowering the pH of the C1 solution, therefore, less (or none) NaOH solution is required to adjust the pH of the C1 solution. Because of this reason, more cobalt ions still remain in the solution while the gel is formed, and more cobalt can be incorporated into the obtained catalysts. In addition, the addition of the acetate salt in either the A1 or the C1 solution results in the same amount of cobalt can be incorporated.

Consequently, in our experimental, cobalt acetate tetrahydrate is the best salt that can incorporate the very most of loaded cobalt into framework. Because of the higher pH value (pH=7) in acetate salt, it is easily to maintain the pH of the mixed solution within 9-11 in preparing step that is a good condition for cobalt incorporate into catalyst and catalyst forming. Moreover, the high pH value causes the decreasing of the amount of NaOH solution that uses to maintain pH during mixing step. Due to the more OH^- addition, the catalyst has irregularly shaped crystal. The chloride salt is better cobalt adding than nitrate salt because of its higher pH value. Hence, the high pH value as a base is suitable for cobalt loading.

5.1.2 Morphology

Morphology of Co-TS-1 catalysts were analyzed by Scanning Electron Microscopy (SEM). These results are presented in Figures 5.2a-5.2j.

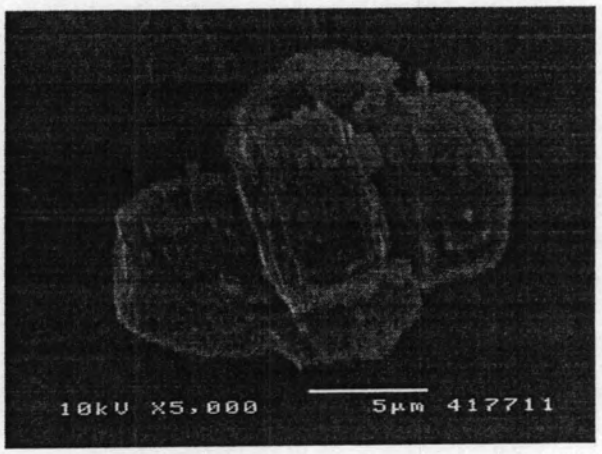

Figure 5.2a SEM photo of Co-TS-1 ($Co(NO_3)_2 \cdot 6H_2O$ loading to A1)

Figure 5.2b SEM photo of Co-TS-1 ($Co(NO_3)_2 \cdot 6H_2O$ loading to A2)

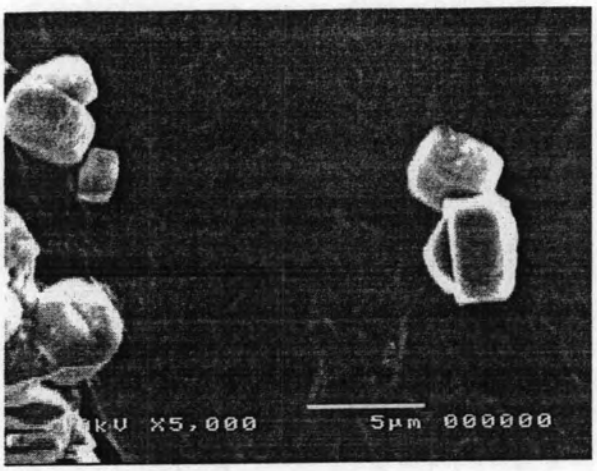

Figure 5.2c SEM photo of Co-TS-1 ($Co(NO_3)_2 \cdot 6H_2O$ loading to C1)

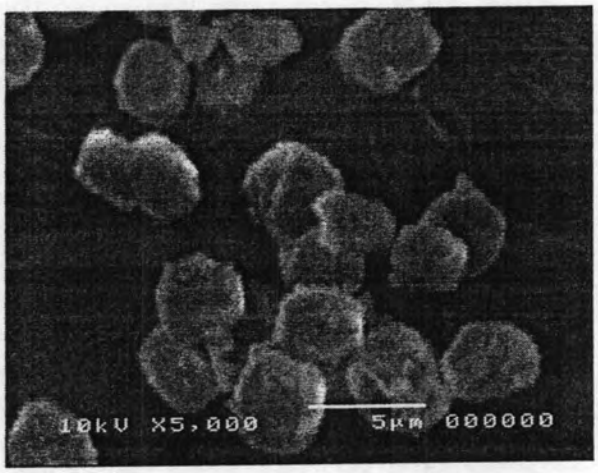

Figure 5.2d SEM photo of Co-TS-1 ($Co(NO_3)_2 \cdot 6H_2O$ loading to A1 and A2)

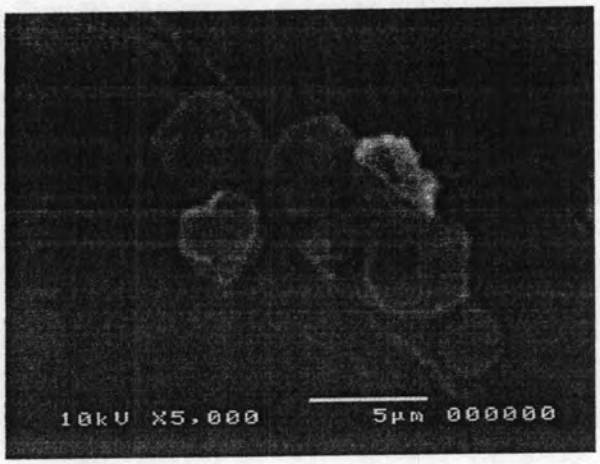

Figure 5.2e SEM photo of Co-TS-1 ($CoCl_2 \cdot 6H_2O$ loading to A1)

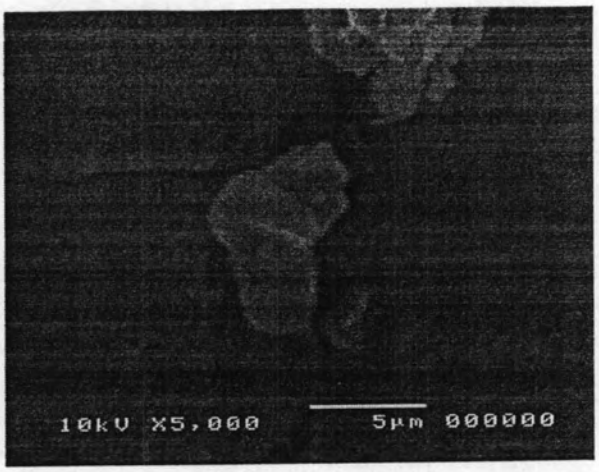

Figure 5.2f SEM photo of Co-TS-1 ($CoCl_2 \cdot 6H_2O$ loading to C1)

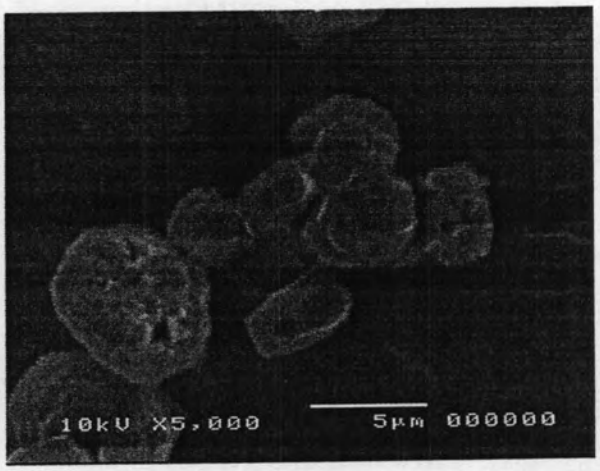

Figure 5.2g SEM photo of Co-TS-1 ($CoCl_2 \cdot 6H_2O$ loading to A1 and A2)

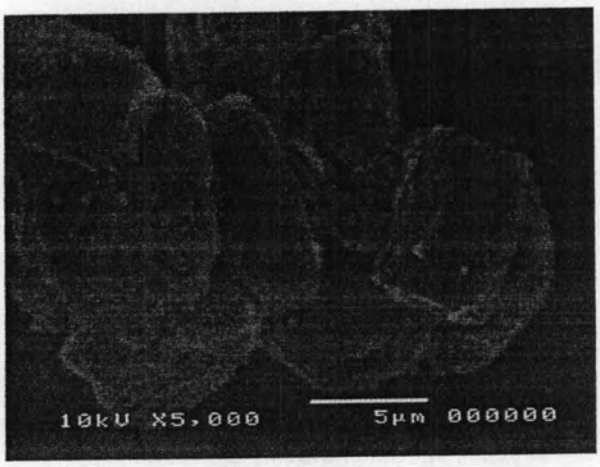

Figure 5.2h SEM photo of Co-TS-1 ($Co(C_2H_3O_2)_2 \cdot 4H_2O$ loading to A1)

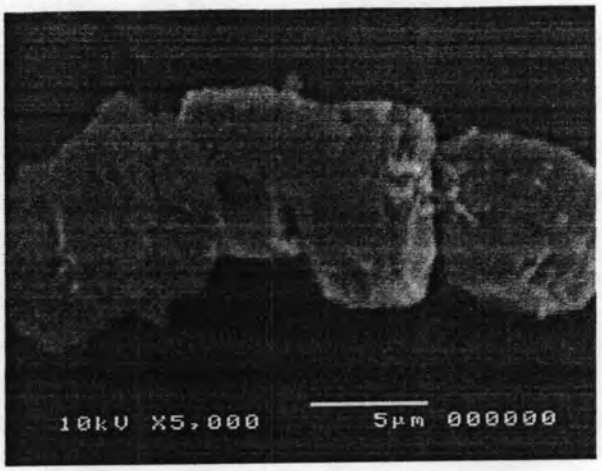

Figure 5.2i SEM photo of Co-TS-1 ($Co(C_2H_3O_2)_2 \cdot 4H_2O$ loading to C1)

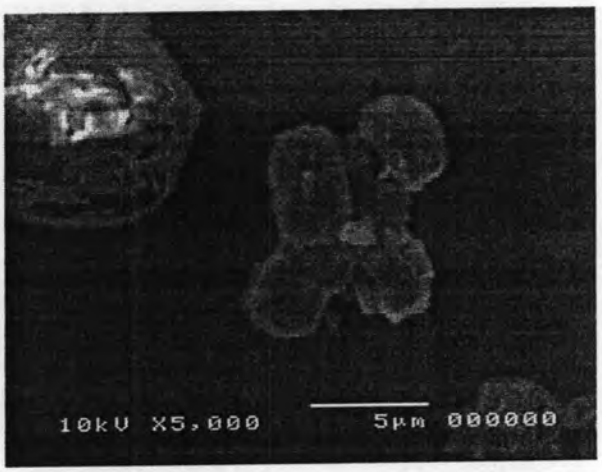

Figure 5.2j SEM photo of Co-TS-1 ($Co(C_2H_3O_2)_2 \cdot 4H_2O$ loading to A1 and A2)

From all of SEM photos as shown, the shapes of all the synthesized samples are crystallized orthorhombic shapes which are composed of many small regular plates. Figures 5.2e-5.2g display a rather uniform crystalline morphology with sizes in range 3-5 μm of Co-TS-1 catalyst that are incorporated with cobalt (II) chloride hexahydrate in A1, C1 and A1A2 solutions, respectively. In contrast, the other Figures 5.2a-5.2c and Figures 5.2h-5.2i show a quite roughly crystalline shape in the bigger particle sizes (5-7 μm) that are loaded with cobalt (II) nitrate hexahydrate and cobalt (II) acetate tetrahydrate, respectively. From the Figures 5.2d, 5.2g, 5.2j, the cobalt loaded in both A1 and A2 solutions exhibit a slightly small particle size (3-5 μm). The reason may depend on the small amount of cobalt metal in catalyst (result from Table 4.1). Since the amount of loaded metals, titanium and cobalt, are so small,

and SiO_2 which is major part of Co-TS-1 samples clearly demonstrates its morphology. As a result, it can refer that the shape and the size of all samples depend on the types of salts (nitrate, acetate, chloride) and the amount of metal that are incorporated during the catalyst preparation.

5.1.3 Crystalline structure

Crystalline structures of all the synthesized catalyst were investigated by powder x-ray diffraction technique, XRD. Figures 5.3a–5.3c show the XRD patterns of Co-TS-1 catalysts. The XRD patterns show six main characteristic peaks at 2θ as 8, 8.8, 14.8, 23.1, 24 and 29.5 degree, marked with dark circle which indicate the MFI structure appear in all of the synthesized samples. The pattern obtained is the pattern typical for a crystalline zeolite having a MFI structure [The JCPDS (1996)]. The catalyst contained a well-defined single-phase XRD pattern and was consistent to those already reported for TS-1 [Taramasso et al. (1983)]. The incorporation of Ti^{4+} into the framework is indicated by the conversion of the monoclinic structure of silicalite-1 to an orthorhombic structure, evidenced by the disappearance of peaked splittings at $2\theta = 24^{\circ}$ and $2\theta = 29.5^{\circ}$ [Taramasso et al. (1983)]. Because of the low Ti content in the support materials (Ti < 3 wt%), additional TiO_2 crystalline phases, i.e., anatase ($2\theta = 25.5^{\circ}$) and rutile ($2\theta = 48.2^{\circ}$) [Yap et al. (2004)], did not appear in the XRD pattern.

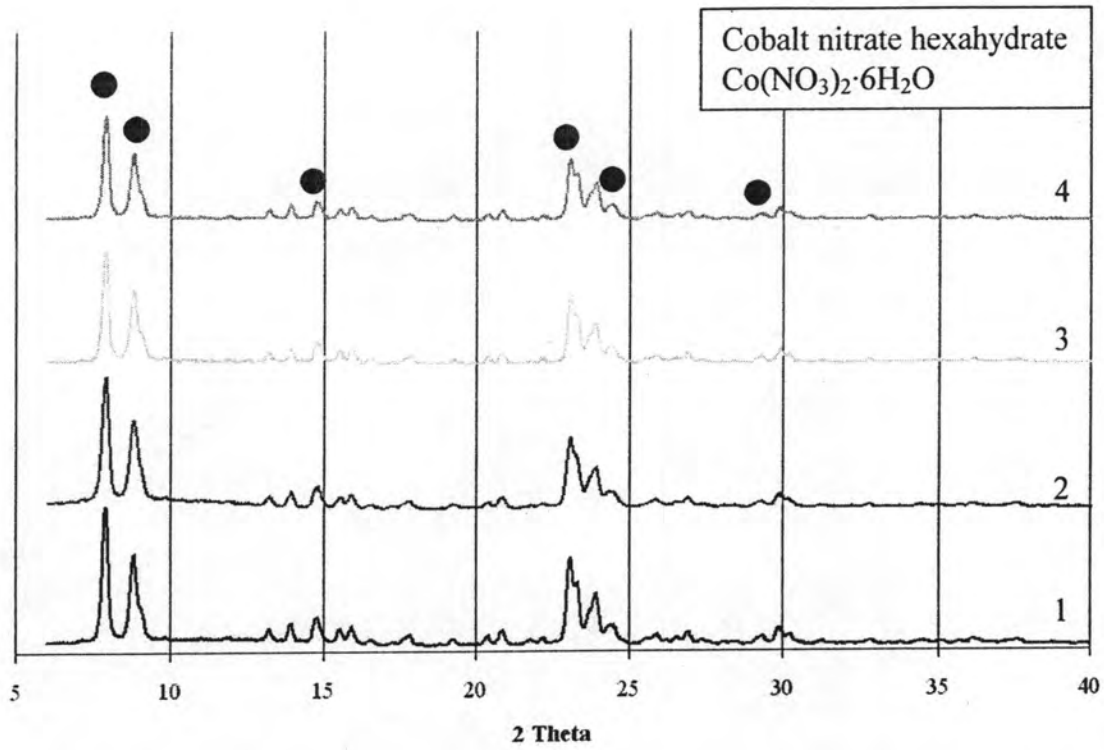

Figure 5.3a XRD spectra of the Co-TS-1 catalyst which used $Co(NO_3)_2 \cdot 6H_2O$ as cobalt salt (loaded in A1 (1), loaded in A2 (2), loaded in C1 (3) and loaded in A1A2 (4)).

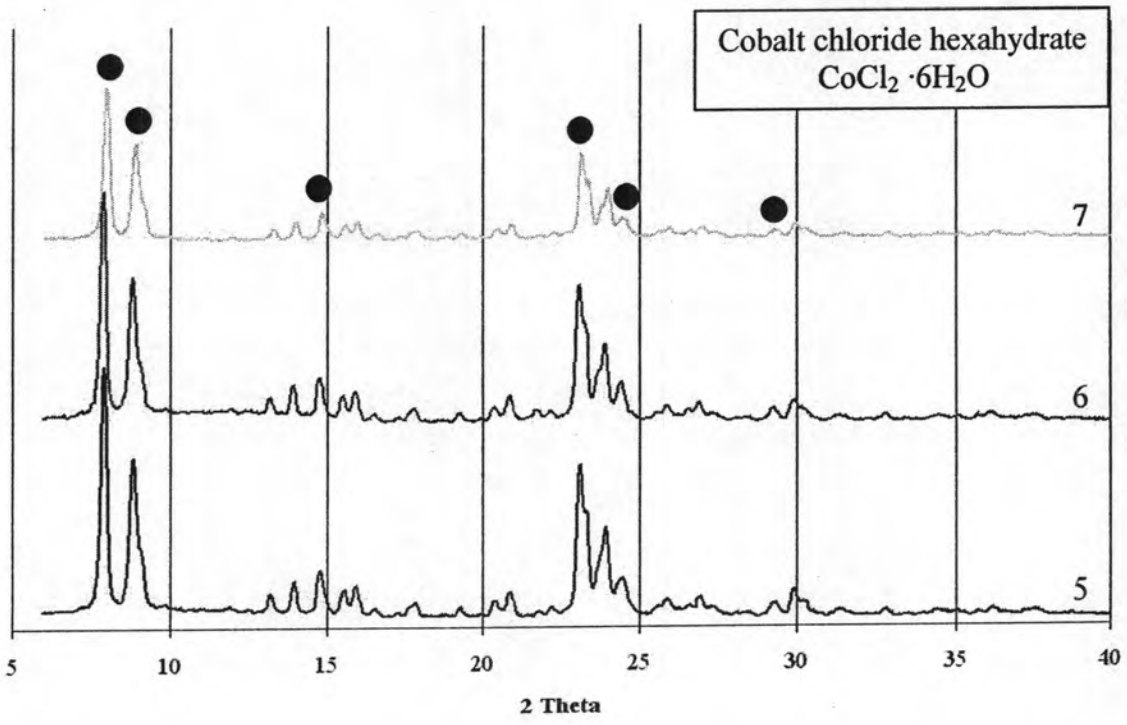

Figure 5.3b XRD spectra of the Co-TS-1 catalyst which used $CoCl_2 \cdot 6H_2O$ as cobalt salt (loaded in A1 (5), loaded in C1 (6) and loaded in A1A2 (7)).

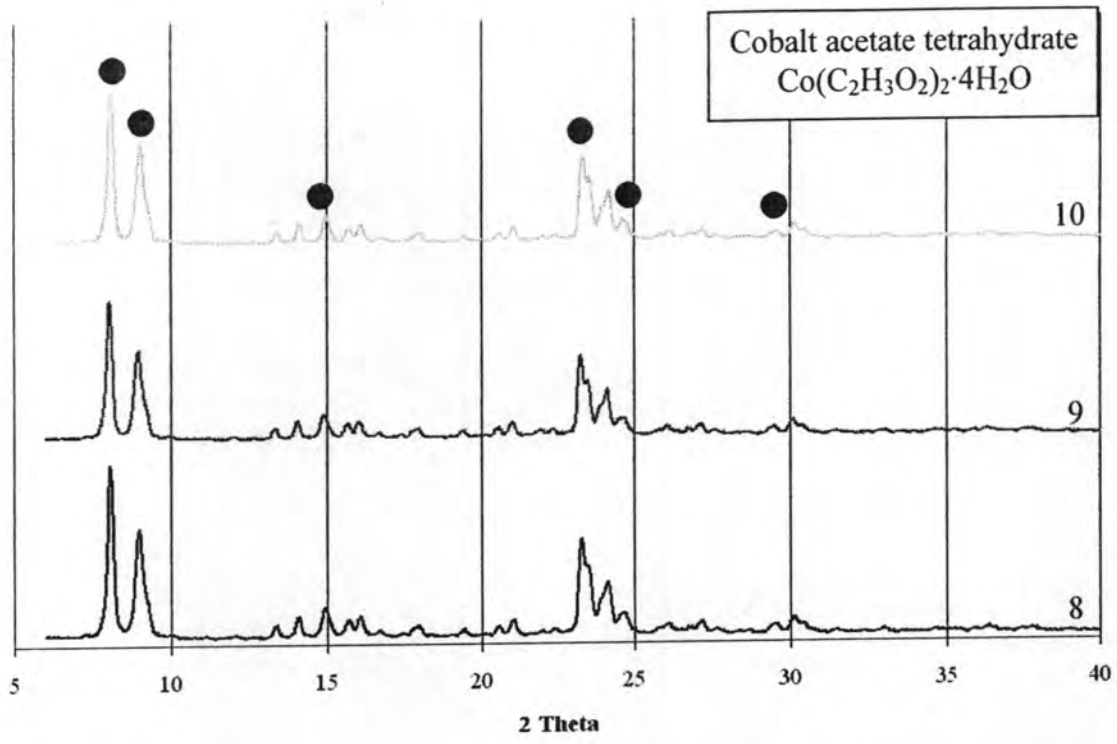

Figure 5.3c XRD spectra of the Co-TS-1 catalyst which used $Co(C_2H_3O_2)_2 \cdot 4H_2O$ as cobalt salt (loaded in A1 (8), loaded in C1 (9) and loaded in A1A2 (10)).

The results show that the XRD pattern of the synthesized Co-TS-1 catalysts, which varies types of salts (nitrate, acetate, chloride) and loading solutions (A1, A2, C1, and C2 solutions which identified in chapter IV) indicates that the different amounts of incorporated cobalt does not affect on the MFI framework and does not change the main structure of MFI. Hence, our synthesized samples have the same XRD patterns that mean the MFI phase with good crystallinity, no other diffraction peaks for contaminating crystalline zeolite and for non-zeolitic phase were detected.

5.1.4 BET surface area, pore volume and pore size of the synthesized Co-TS-1 catalyst

The summary of the surface area, pore volume and pore size distribution of the samples (Co-TS-1), were determined by the adsorption and condensation of N_2 at liquid N_2 boiling point temperature (-196 °C) using static vacuum procedure. This technique is called "BET" method according to the inventor's name (Bruanauer, Emmett and Teller). The measured values of all samples are reported in Table 5.2.

Table 5.2 BET surface area, pore volume and average pore size of the synthesized Co-TS-1 samples.

Sample	Types of Salts	Loading Solution	BET Surface (m^2/g)	Pore Volume (ml/g)	Pore Size (Å)
batch 1	$Co(NO_3)_2 \cdot 6H_2O$	A1	314.837	0.149	34.610
batch 2		A2	305.260	0.147	33.381
batch 3		C1	344.180	0.178	36.941
batch 4		A1 and A2	308.785	0.158	38.402
batch 5	$CoCl_2 \cdot 6H_2O$	A1	296.585	0.142	39.834
batch 6		C1	290.529	0.134	41.725
batch 7		A1 and A2	298.904	0.156	41.091
batch 8	$Co(C_2H_3O_2)_2 \cdot 4H_2O$	A1	324.514	0.194	44.235
batch 9		C1	308.285	0.154	37.857
batch 10		A1 and A2	321.788	0.148	38.417

From Table 5.2, the incorporated cobalt catalysts which various types of cobalt salts (nitrate, acetate, chloride) have an proximity in the BET surface area, pore volume and pore size. The BET surface area, pore volume and pore size of nitrate salts catalyst are around the value of acetate salts catalyst in the range of 305-344 m^2/g, 0.14-0.19 ml/g and 33-44 Å, respectively.

On the other hand, we can see that the chloride salt catalyst cause a slightly smaller in surface area and pore volume than the other salts, although the morphology of chloride loaded catalysts have a smaller particle size. Another result about the effect of the loading solutions (A1, A2, C1 and C2 solutions) shows that the loaded cobalt in each solution with the same salt has negligible changes in both the surface area and porosity. It indicates that the concentration of cobalt salts does not cause any further change in the property of this cobalt containing samples.

Consequently, the Co-TS-1 catalysts prepared with various cobalt salts and incorporated in each solution have negligible changes in among BET surface area,

pore volume and pore size distribution. Because the catalysts mainly consisted of SiO_2 and low amount of loaded transitions metal therefore, SiO_2 plays an important role on the physical properties of catalysts. Hence, the BET surface area, pore volume and pore size are hardly depend on the amount of cobalt that incorporated in TS-1 framework.

5.1.5 The functional group in the catalysts

To investigate the existence of framework titanium, Fourier Transform Infrared Spectroscopy, FT-IR, was used in our study. It is well known that the vibrational spectrum of TS-1 is characterized by an absorption band in the 900-975 cm^{-1} region [Taramasso et al. (1983)]. The presence peak around 960-975 cm^{-1} indicated that Ti^{4+} exist in silicate framework [Huybrechts et al. (1991)]. Another research of Li et al. (1998) and Bellussi et al. (1991) indicated that the band at 960 cm^{-1} is commonly accepted as the characteristic asymmetric Ti-O-Si stretching mode of Ti- and Si- containing catalysts. In the present case, is the fingerprint of titanium incorporated into the MFI structure. IR Spectroscopy may be used to prove that the Ti has enters the silicalite lattice [Zecchina et al. (1991)], since an additional band typical for tetrahedral group $Ti(OSi)_4$ appear in the silicalite spectrum at 960 cm^{-1}.

In our experiment, the spectra of all samples were measured around 400-1200 cm^{-1} by FT-IR. These results are represented by Figures 5.4a-5.4c.

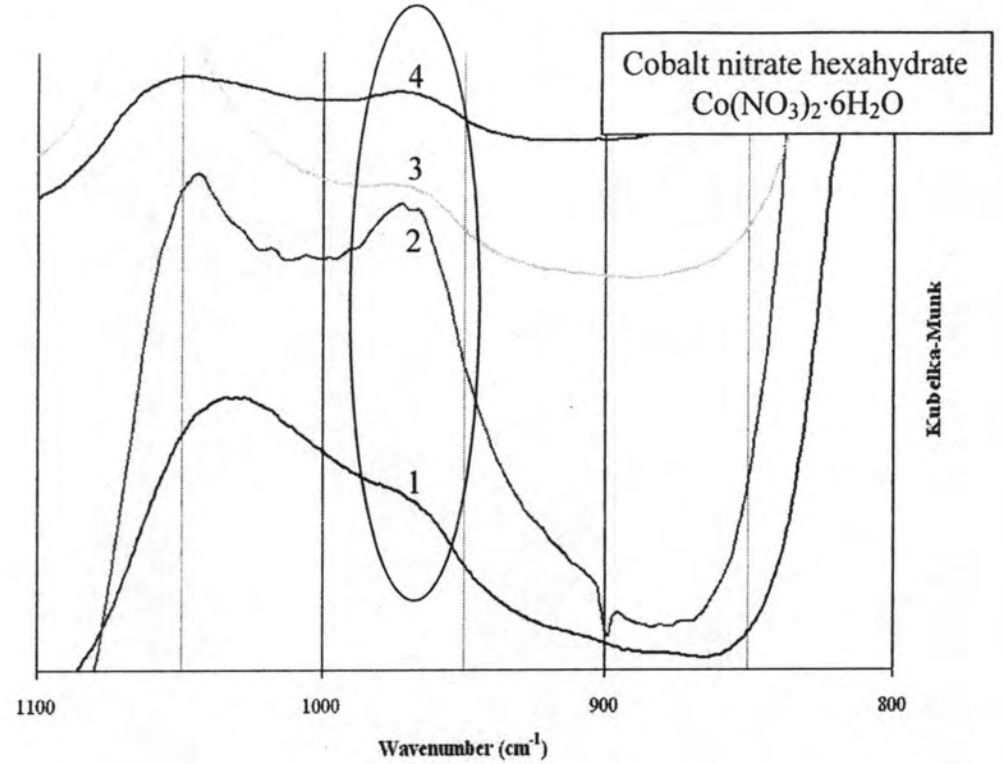

Figure 5.4a IR spectra of the synthesized Co-TS-1 catalyst which used $Co(NO_3)_2 \cdot 6H_2O$ as cobalt salt (loaded in A1 (1), loaded in A2 (2), loaded in C1 (3) and loaded in A1A2 (4)).

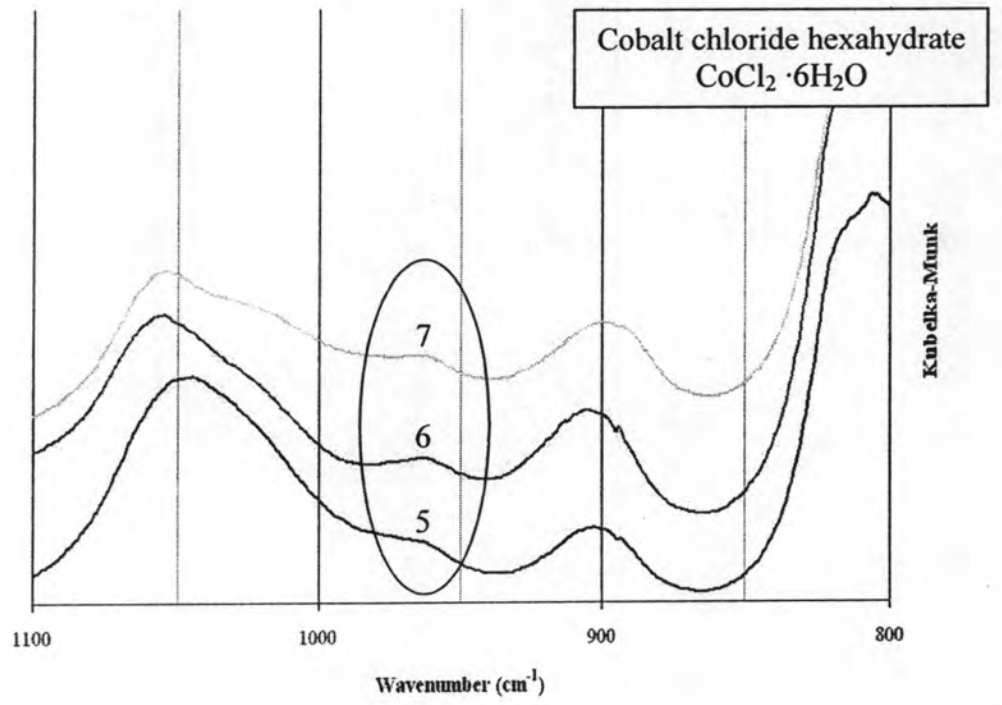

Figure 5.4b IR spectra of the synthesized Co-TS-1 catalyst which used $CoCl_2 \cdot 6H_2O$ as cobalt salt (loaded in A1 (5), loaded in C1 (6) and loaded in A1A2 (7)).

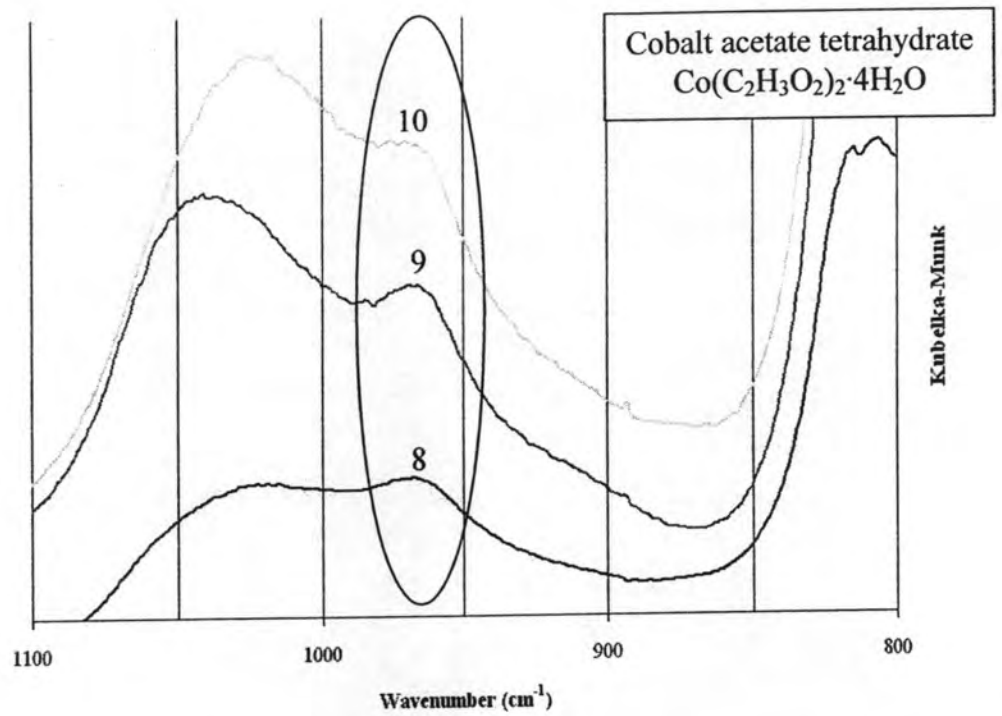

Figure 5.4c IR spectra of the synthesized Co-TS-1 catalyst which used $Co(C_2H_3O_2)_2 \cdot 4H_2O$ as cobalt salt (loaded in A1 (8), loaded in C1 (9) and loaded in A1A2 (10)).

From Figures 5.4a-5.4c, IR spectra of Co-TS-1 catalysts exhibit the absorption band around 960-970 cm^{-1}. It is associated with the presence of titanium in the lattice of silicalite and is an indication for the formation of TS-1 crystals and the amounts of cobalt on TS-1 are much less to observe the changes in IR bands.

5.1.6 Acid quantities and acid strength

Most of reactions occur at catalyst surface; therefore, the investigation of active site on catalyst surface is useful for interpretation of reaction pathway. In our study, two main reactions, selective oxidation and dehydration need active sites being acid. Hence, we investigated the active site of our synthesized catalysts by explore acid site on the catalyst surface.

Ammonia temperature programmed desorption (NH_3-TPD) characterization was conducted to survey the acid sites and acid strength on the catalyst surface and the influence of cobalt loading on it.

The results are shown in Table 5.3 which is calculated from raw data of NH_3-TPD with some helps of peak fitting program (fityk program) as shown in Appendix D. The details of each NH_3-TPD profile are shown in Figures 5.5a-5.5j and data of acid quantities and acid strength from the fityk program are shown in Tables 5.4a-5.4j.

The Co-TS-1 synthesized in this study with difference cobalt salts ($Co(NO_3)_2 \cdot 6H_2O$, $CoCl_2 \cdot 6H_2O$, $Co(C_2H_3O_2)_2 \cdot 4H_2O$) and loading solutions (A1, A2, C1 and A1A2) showed almost the same TPD signals. It can be seen that peaks appeared only in the temperature region 100-300 °C. The profile of NH_3-TPD is composed of two main peaks: a low temperature peak corresponding to weaker acid sites, appear around 133-153 °C and a high temperature peak corresponding to stronger acid sites, appear around 213-249°C. The peak area and peak temperature reflect the acid sites and acid strength, respectively.

From Table 5.3 shows the acid strength (the top peak temperature) on the surface of each catalyst samples changed hardly, but the acid amount (the peak area) increased slightly with cobalt increasing. The acid strength of the peak, both weaker and stronger acid sites, is slightly offset. The discrepancy is the area under the peaks, i.e. the amount of acid site. These results indicate that the cobalt loading into TS-1 framework causes the ratio of strong acid sites increase rather than the ratio of weak acid sites on the surface of catalyst. For this reason, the raise of total acid sites occurred. Therefore, the amount of cobalt in TS-1 framework also relates to the number of the total acid site in the same direction. The acid amount of total acid sites of catalysts are found around 122-256 μmol/g. As a result, the minimum and maximum of weaker and total acid sites are Co-TS-1 (batch 2) and Co-TS-1 (batch9) that have minimum and maximum amount of cobalt, respectively.

Comparison between Co-TS-1 (batch 2) and the other samples, it should be noted that the amount of Co in batch 2 are rarely exist. Co-TS-1 (batch 2) catalyst had a lower high temperature peak (weaker acid sites) at the lower temperature range than other samples, indicating that the strength of weaker acid site of Co-TS-1 (batch 2) was much weaker than of others.

It is clearly seen that the number of Ti^{4+} in the silicalite framework relates to the number of stronger acid. The ratio of stronger acid sites on the catalyst surface is increased with more Ti^{4+} in the silicalite framework of Co-TS-1 samples except Co-TS-1 (batch 2) which does not have cobalt metal in the sample. As a result Ti^{4+} in the silicate framework causes the stronger acid sites on the catalyst surface increase.

Consequently, the added cobalt has significant effect on the amount of surface acidity of TS-1 but slightly effect on the strength of catalyst surface.

Table 5.3 Desorption temperature and acid site quantities of the synthesized Co-TS-1 sample with different cobalt salts.

Sample	Types of Salts	Loading Solution	%Ti	%Co	Weaker Acid Site			Stronger Acid Site			Total Acid Site (μmol/g)
					Max Temp. (°C)	Acid Site (μmol/g)	Acid Site (%)	Max Temp. (°C)	Acid Site (μmol/g)	Acid Site (%)	
batch 1	$Co(NO_3)_2 \cdot 6H_2O$	A1	0.24	0.26	147	178.59	74.68	249	60.56	25.32	239.14
batch 2		A2	0.33	0	133	115.83	94.40	224	6.88	5.60	122.71
batch 3		C1	0.21	0.16	142	168.53	74.11	236	58.86	25.89	227.40
batch 4		A1 and A2	0.27	0.11	145	121.52	55.61	235	78.05	44.39	218.52
batch 5	$CoCl_2 \cdot 6H_2O$	A1	0.31	0.26	148	165.63	70.05	243	70.82	29.95	236.45
batch 6		C1	0.31	0.42	144	169.64	66.07	231	87.12	33.93	256.76
batch 7		A1 and A2	0.32	0.13	153	125.33	53.02	243	111.04	46.98	236.37
batch 8	$Co(C_2H_3O_2)_2 \cdot 4H_2O$	A1	0.29	0.40	141	140.62	54.93	213	115.37	45.07	255.99
batch 9		C1	0.33	0.44	140	195.40	76.32	236	60.61	23.68	256.02
batch 10		A1 and A2	0.28	0.20	141	135.59	58.15	228	97.60	41.85	233.19

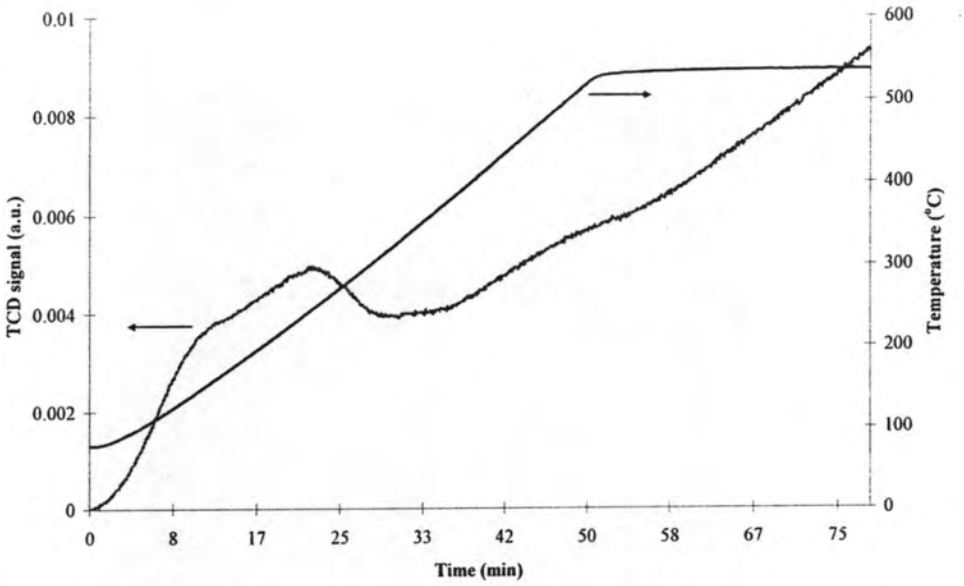

Figure 5.5a-1 The relation of TCD signal, temperature and time of Co-TS-1 ($Co(NO_3)_2 \cdot 6H_2O$ loading to A1)

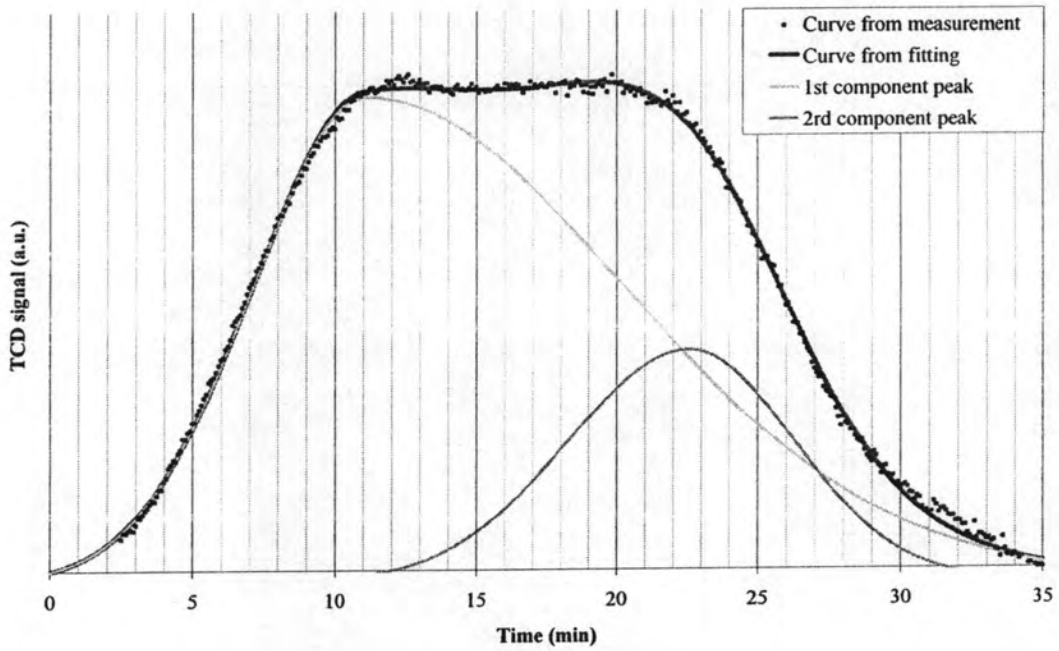

Figure 5.5a-2 The data of peak fitting of Co-TS-1 ($Co(NO_3)_2 \cdot 6H_2O$ loading to A1)

Table 5.4a Data of acid quantities and acid strength

Sample	Time (min)	Temp (°C)	Peak area (area unit)
Co-TS-1 ($Co(NO_3)_2 \cdot 6H_2O$ loading to A1)	11.11	147	0.043
	22.60	249	0.012

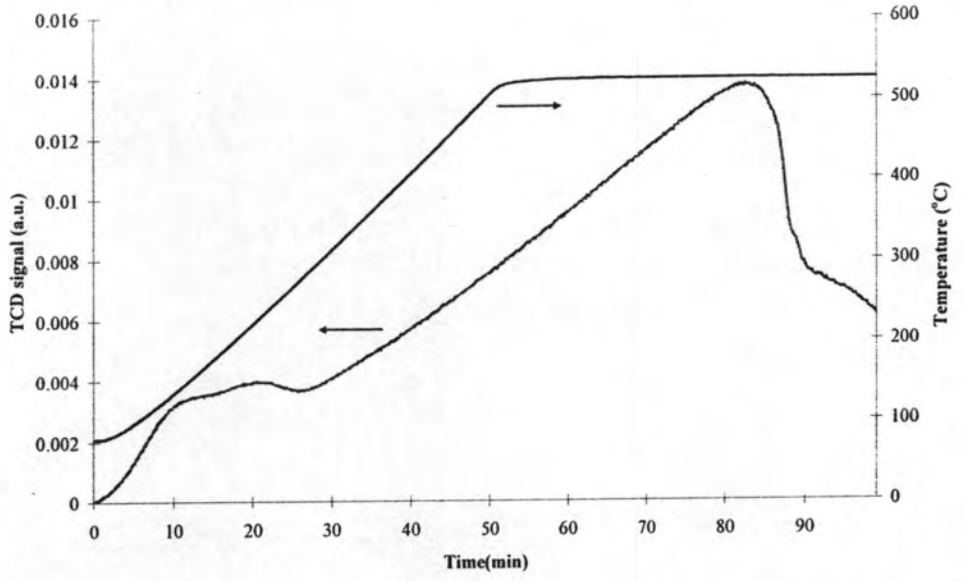

Figure 5.5b-1 The relation of TCD signal, temperature and time of Co-TS-1 ($Co(NO_3)_2 \cdot 6H_2O$ loading to A2)

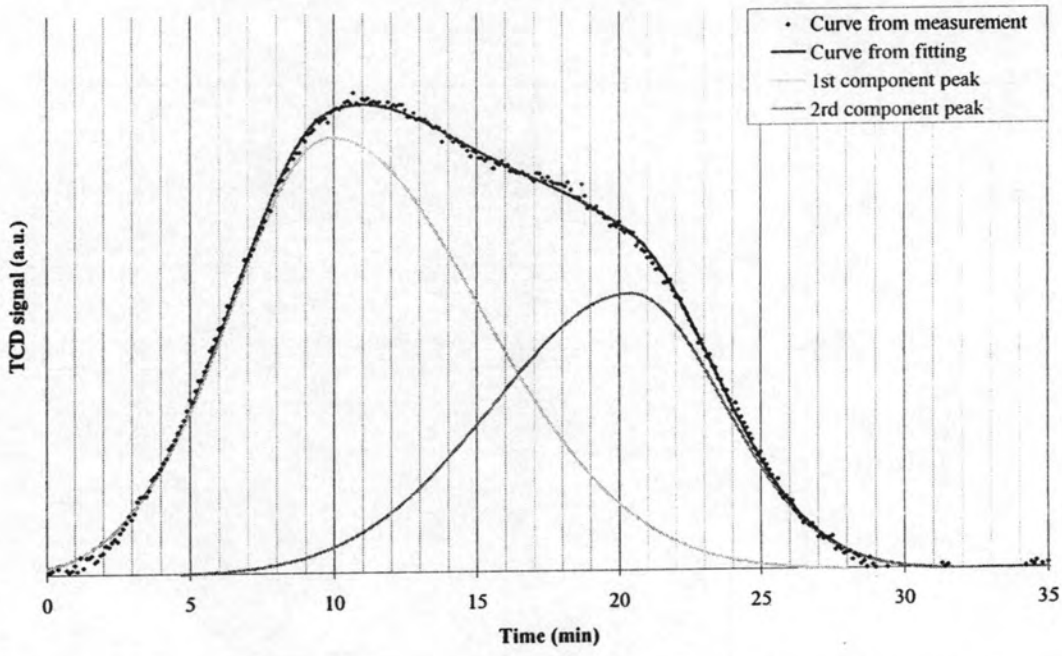

Figure 5.5b-2 The data of peak fitting of Co-TS-1 ($Co(NO_3)_2 \cdot 6H_2O$ loading to A2)

Table 5.4b Data of acid quantities and acid strength

Sample	Time (min)	Temp (°C)	Peak area (area unit)
Co-TS-1 ($Co(NO_3)_2 \cdot 6H_2O$ loading to A2)	9.90	133	0.214
	20.41	224	0.013

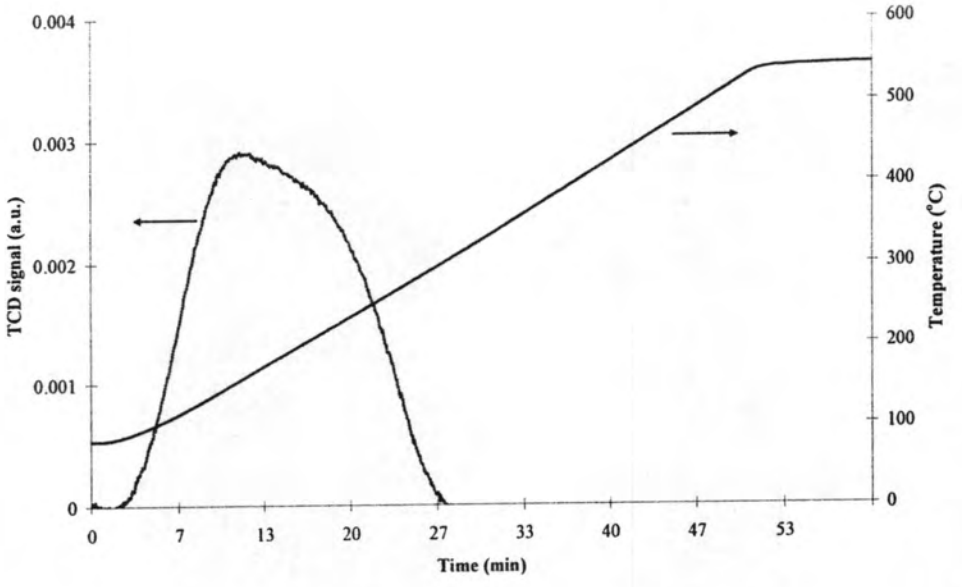

Figure 5.5c-1 The relation of TCD signal, temperature and time of Co-TS-1 ($Co(NO_3)_2 \cdot 6H_2O$ loading to C1)

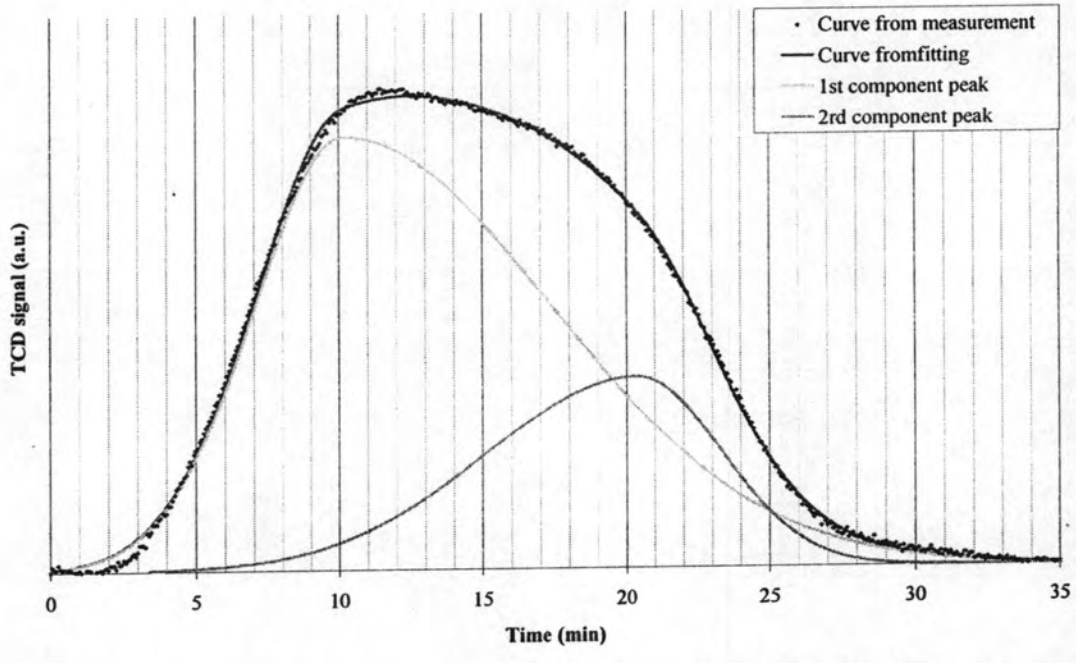

Figure 5.5c-2 The data of peak fitting of Co-TS-1 ($Co(NO_3)_2 \cdot 6H_2O$ loading to C1)

Table 5.4c Data of acid quantities and acid strength

Sample	Time (min)	Temp (°C)	Peak area (area unit)
Co-TS-1 ($Co(NO_3)_2 \cdot 6H_2O$ loading to C1)	10.16	142	0.036
	20.39	236	0.012

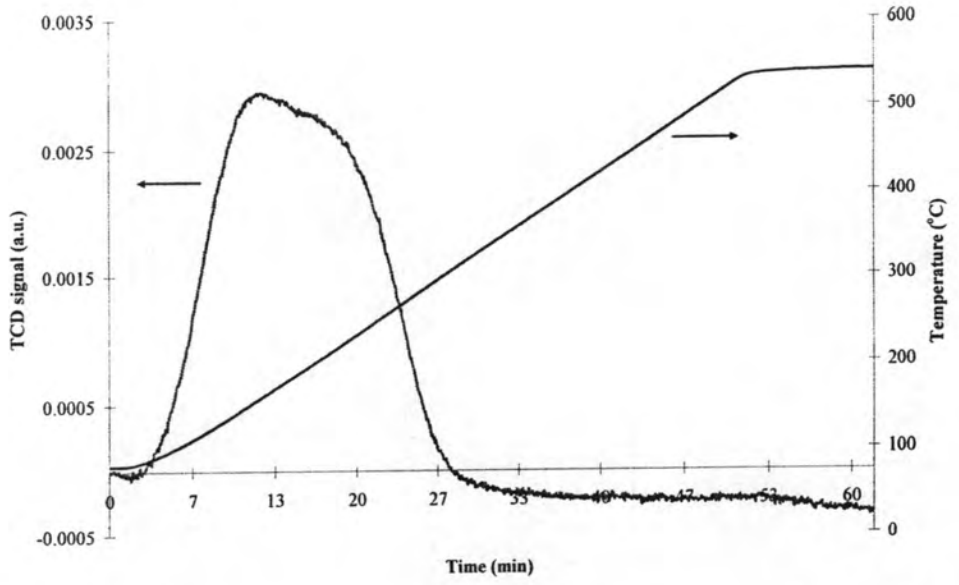

Figure 5.5d-1 The relation of TCD signal, temperature and time of Co-TS-1 ($Co(NO_3)_2 \cdot 6H_2O$ loading to A1 and A2)

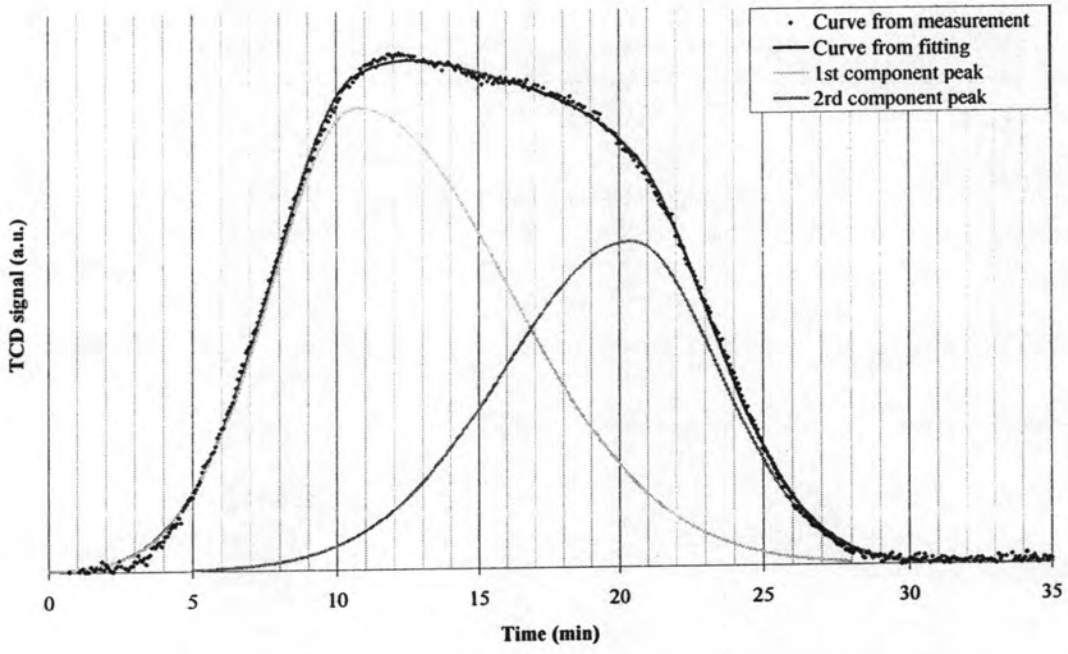

Figure 5.5d-2 The data of peak fitting of Co-TS-1 ($Co(NO_3)_2 \cdot 6H_2O$ loading to A1 and A2)

Table 5.4d Data of acid quantities and acid strength

Sample	Time (min)	Temp (°C)	Peak area (area unit)
Co-TS-1 ($Co(NO_3)_2 \cdot 6H_2O$ loading to A1	10.73	145	0.026
and A2)	20.43	235	0.017

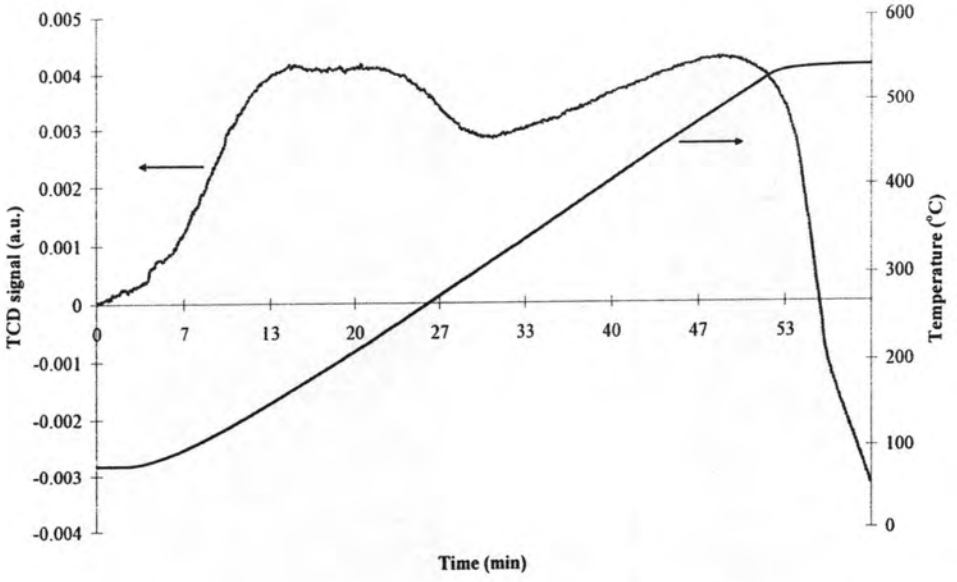

Figure 5.5e-1 The relation of TCD signal, temperature and time of Co-TS-1 ($CoCl_2 \cdot 6H_2O$ loading to A1)

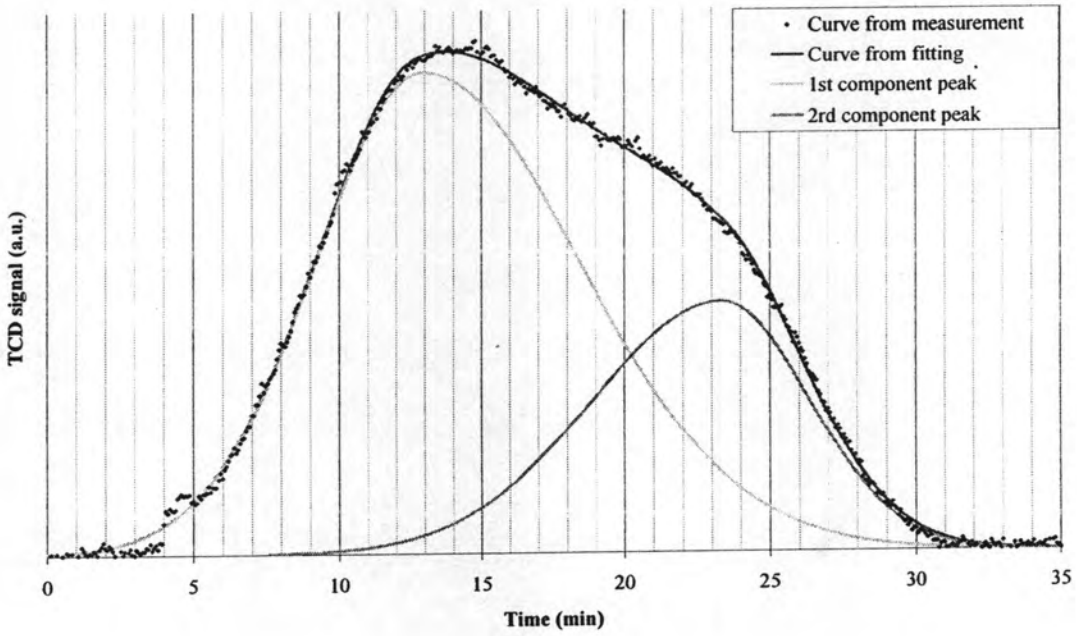

Figure 5.5e-2 The data of peak fitting of Co-TS-1 ($CoCl_2 \cdot 6H_2O$ loading to A1)

Table 5.4e Data of acid quantities and acid strength

Sample	Time (min)	Temp (°C)	Peak area (area unit)
Co-TS-1 ($CoCl_2 \cdot 6H_2O$ loading to A1)	12.95	148	0.031
	23.36	243	0.013

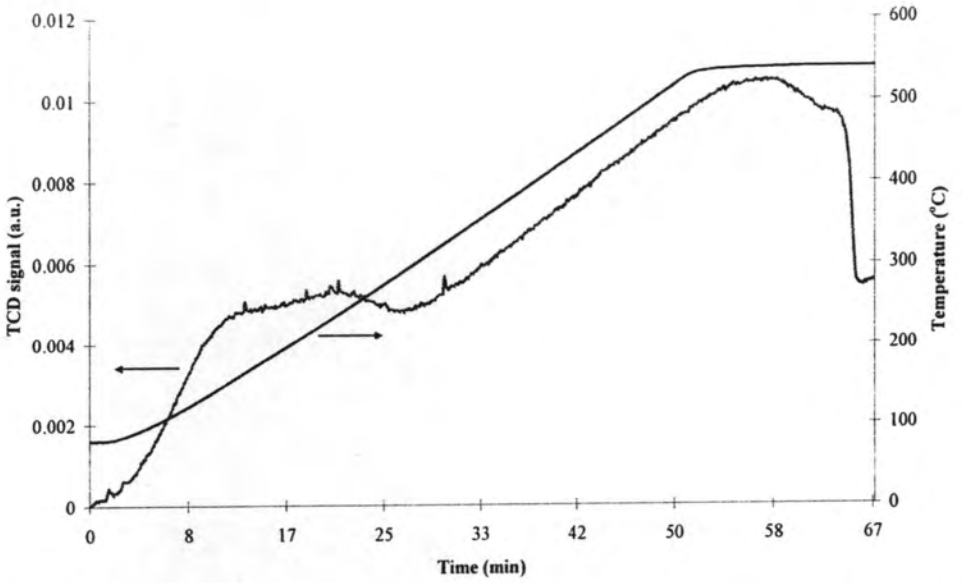

Figure 5.5f-1 The relation of TCD signal, temperature and time of Co-TS-1 ($CoCl_2 \cdot 6H_2O$ loading to C1)

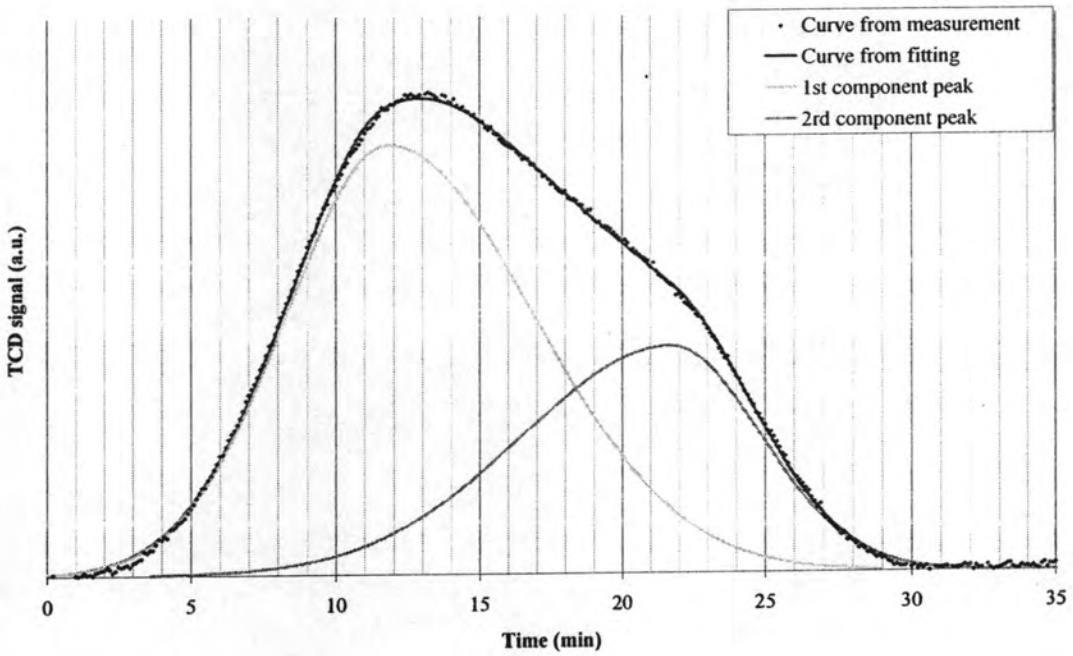

Figure 5.5f-2 The data of peak fitting of Co-TS-1 ($CoCl_2 \cdot 6H_2O$ loading to A1)

Table 5.4f Data of acid quantities and acid strength

Sample	Time (min)	Temp (°C)	Peak area (area unit)
Co-TS-1 ($CoCl_2 \cdot 6H_2O$ loading to C1)	11.83	144	0.033
	21.74	231	0.017

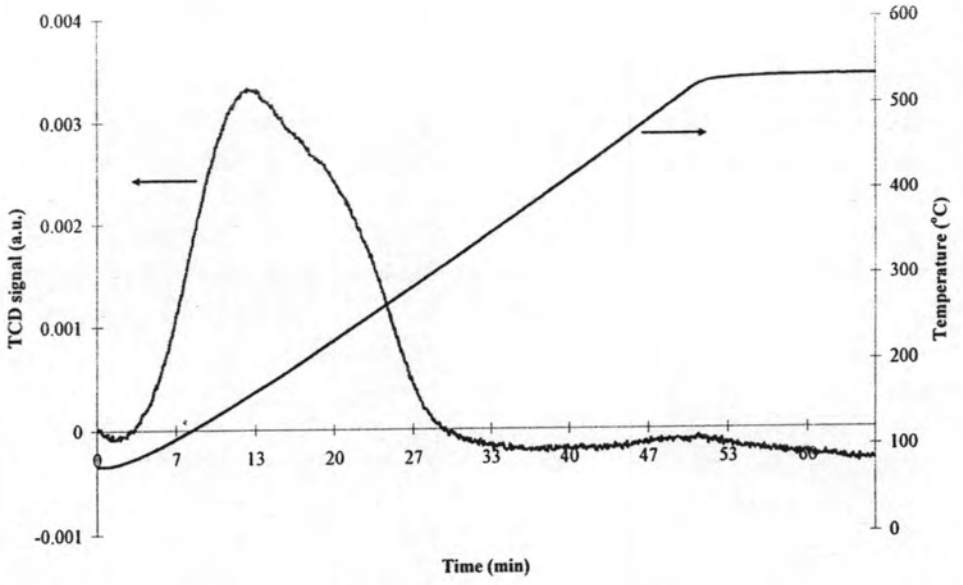

Figure 5.5g-1 The relation of TCD signal, temperature and time of Co-TS-1 ($CoCl_2 \cdot 6H_2O$ loading to A1 and A2)

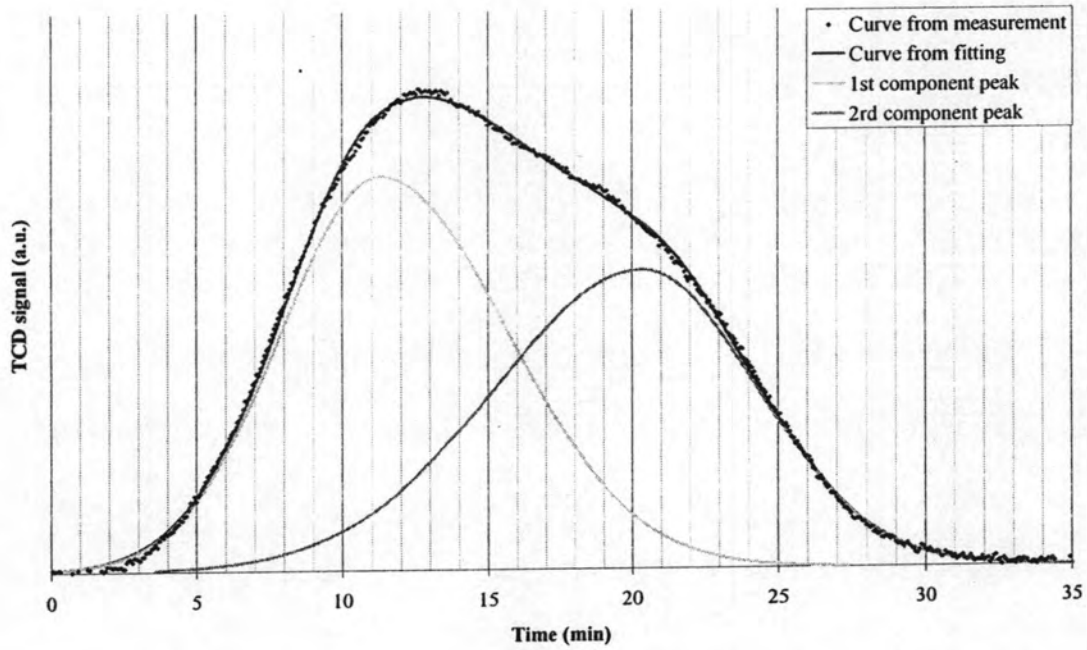

Figure 5.5g-2 The data of peak fitting of Co-TS-1 ($CoCl_2 \cdot 6H_2O$ loading to A1 and A2)

Table 5.4g Data of acid quantities and acid strength

Sample	Time (min)	Temp (°C)	Peak area (area unit)
Co-TS-1 ($CoCl_2 \cdot 6H_2O$ loading to A1 and A2)	11.30	153	0.027
	20.37	243	0.024

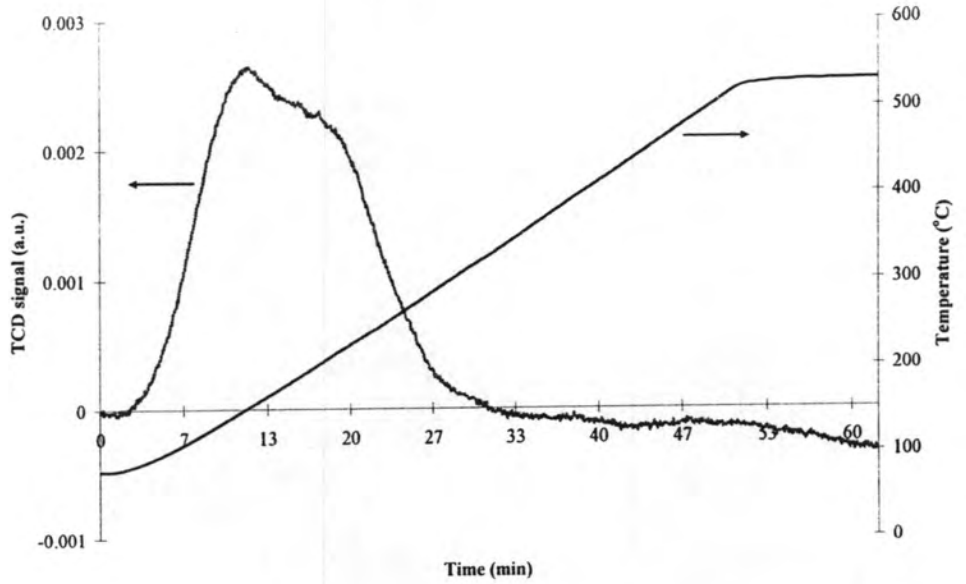

Figure 5.5h-1 The relation of TCD signal, temperature and time of Co-TS-1 ($Co(C_2H_3O_2)_2 \cdot 4H_2O$ loading to A1)

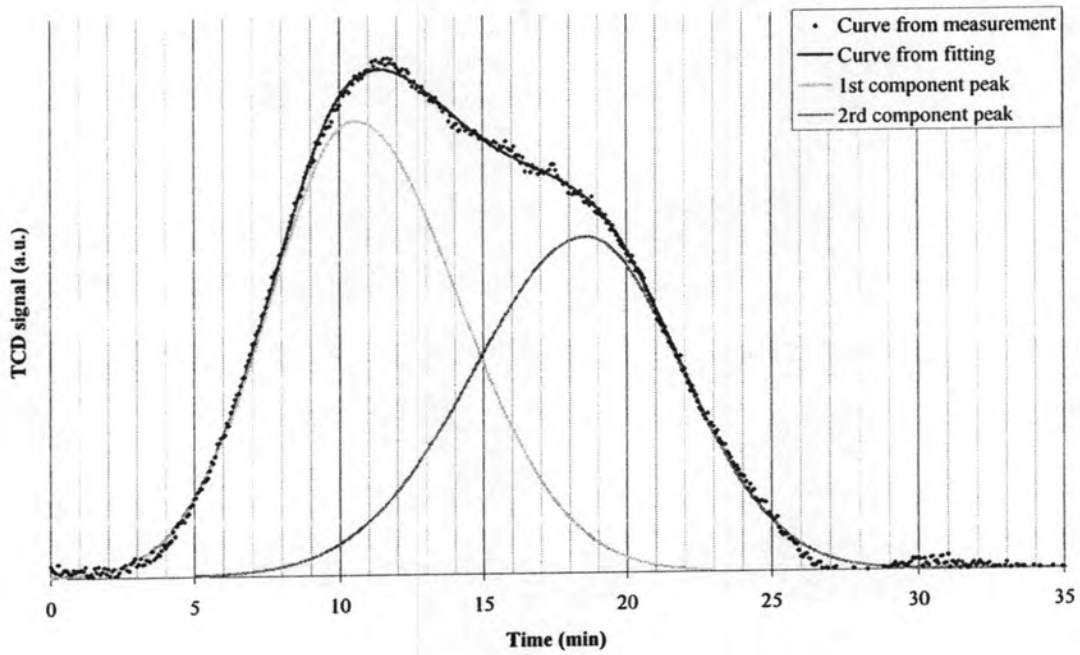

Figure 5.5h-2 The data of peak fitting of Co-TS-1 ($Co(C_2H_3O_2)_2 \cdot 4H_2O$ loading to A1)

Table 5.4h Data of acid quantities and acid strength

Sample	Time (min)	Temp (°C)	Peak area (area unit)
Co-TS-1 ($Co(C_2H_3O_2)_2 \cdot 4H_2O$ loading to A1)	10.51	141	0.017
	18.61	213	0.014

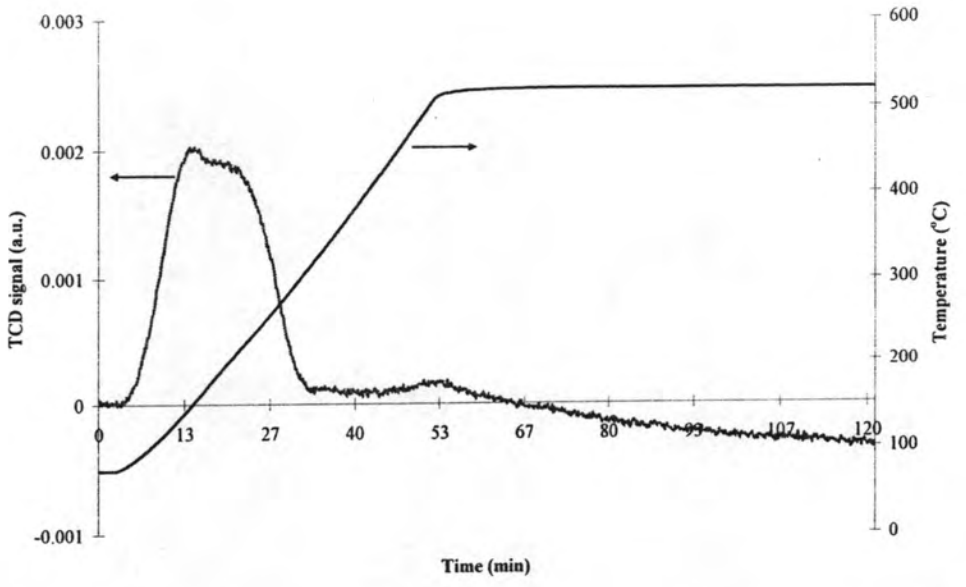

Figure 5.5i-1 The relation of TCD signal, temperature and time of Co-TS-1 ($Co(C_2H_3O_2)_2 \cdot 4H_2O$ loading to C1)

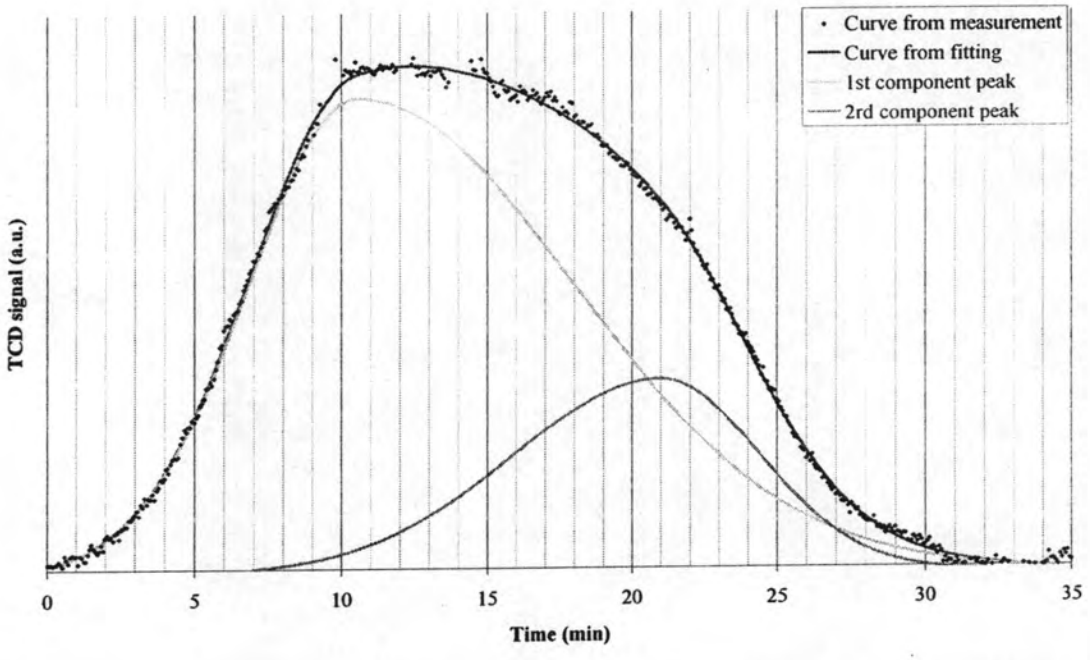

Figure 5.5i-2 The data of peak fitting of Co-TS-1 ($Co(C_2H_3O_2)_2 \cdot 4H_2O$ loading to C1)

Table 5.4i Data of acid quantities and acid strength

Sample	Time (min)	Temp (°C)	Peak area (area unit)
Co-TS-1 ($Co(C_2H_3O_2)_2 \cdot 4H_2O$ loading to C1)	10.53	140	0.030
	21.01	236	0.009

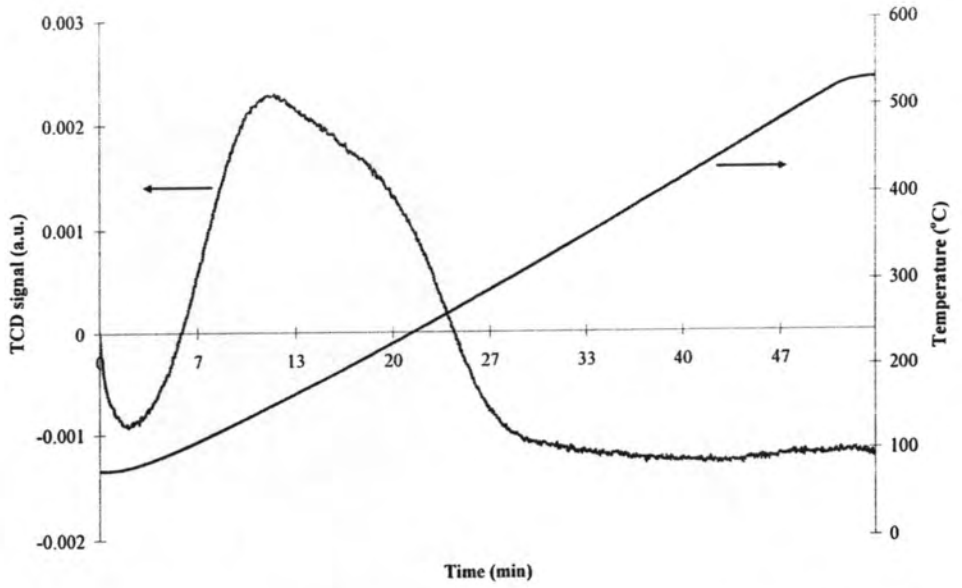

Figure 5.5j-1 The relation of TCD signal, temperature and time of Co-TS-1 ($Co(C_2H_3O_2)_2 \cdot 4H_2O$ loading to A1 and A2)

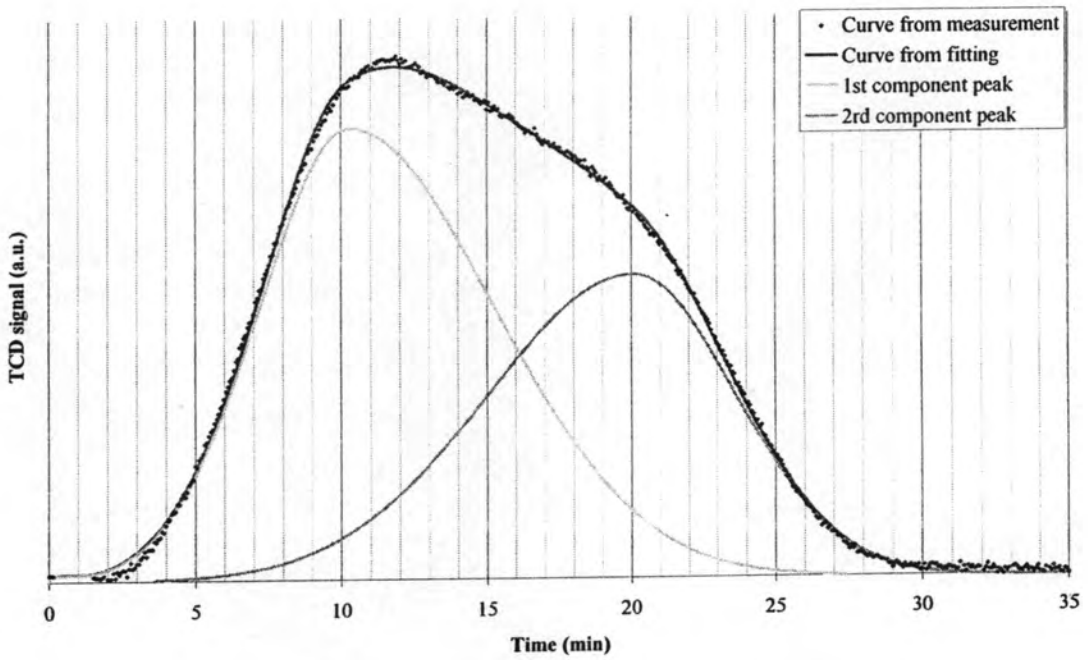

Figure 5.5j-2 The data of peak fitting of Co-TS-1 $Co(C_2H_3O_2)_2 \cdot 4H_2O$ loading to A1 and A2)

Table 5.4j Data of acid quantities and acid strength

Sample	Time (min)	Temp (°C)	Peak area (area unit)
Co-TS-1 $Co(C_2H_3O_2)_2 \cdot 4H_2O$ loading to A1 and A2)	10.28	141	0.029
	20.08	228	0.021

5.2 Catalytic reaction of 2-propanol oxidation

In this part, the catalytic properties of Co-TS-1 catalysts are tested by using the 2-propanol oxidation reaction which composes of 5% 2-propanol and 8% oxygen in our system at 100-500°C and 1 atm. The collected sample was analyzed with gas chromatography, GC, technique described in Chapter IV. The raw data from GC results were converted to moles of products, conversion and selectivity values as showed in Appendix E.

The grams mole of product from our reaction tests which used $Co(NO_3)_2 \cdot 6H_2O$ as cobalt salts loaded in A1 solution is showed in Figure 5.6 and other results are showed in Appendix E. The conversion and selectivity of Co-TS-1 samples with different cobalt salts (nitrate, chloride, acetate) and loading solution are showed in Figures 5.8a-5.8j.

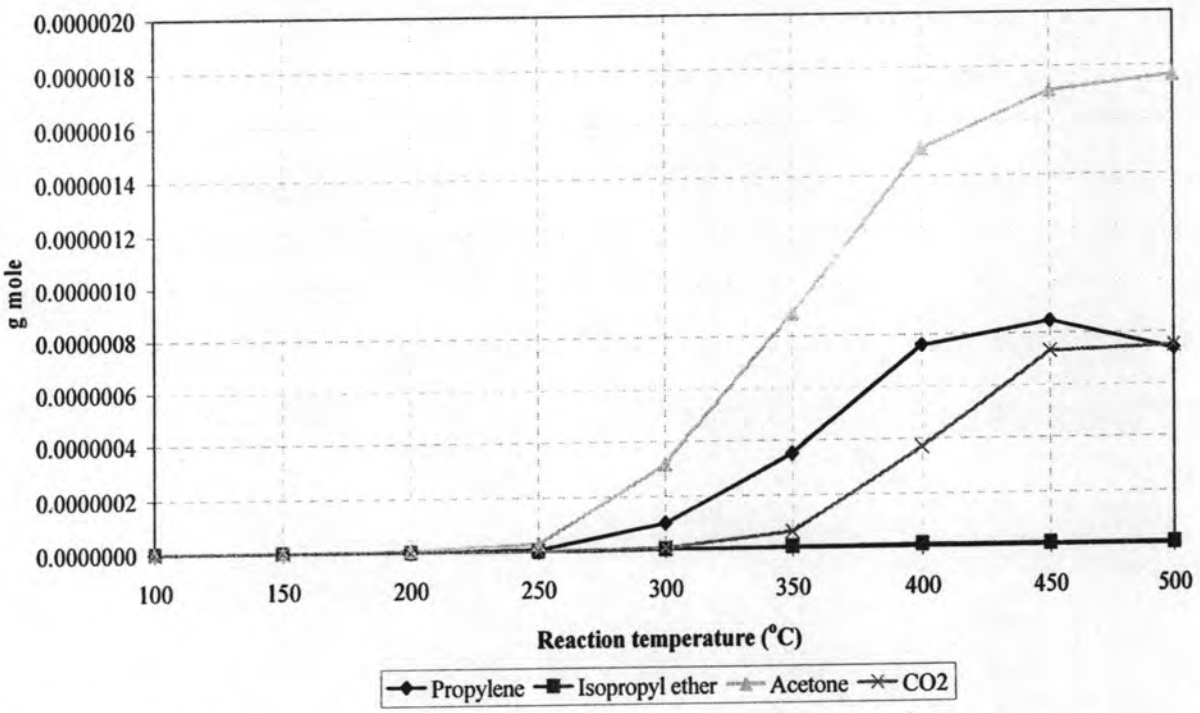

Figure 5.6 The amount of product of 2-propanol over Co-TS-1 for 8 Vol% O_2 system ($Co(NO_3)_2 \cdot 6H_2O$ loading to A1).

Form the results of Figure 5.6, the reaction of Co-TS-1 catalyst produced four types of products: acetone, propylene, carbon dioxide and isopropyl ether. Because of so slightly amount of isopropyl ether (product of the dehydration between two 2-propanol

molecules), the formation of isopropyl ether, therefore, will not be considered in the further discussion. For this reason, this experiment only interested in three main products that play an important role on the 2-propanol oxidation reaction.

Hence, the reaction involved in three reactions; selective oxidation, dehydration and combustion reactions. In the experiment, the selective oxidation ability of the synthesized catalyst was evaluated by the selectivity of acetone. In addition, dehydration ability and combustion ability were evaluated by the selectivities of propylene and carbon dioxide, respectively.

The pathway of product formation in 2-propanol oxidation reaction on Co-TS-1 catalysts can be summarized in Figure 5.7 which is as same as the pathway of TS-1 catalyst that ever present by Chairut (2004).

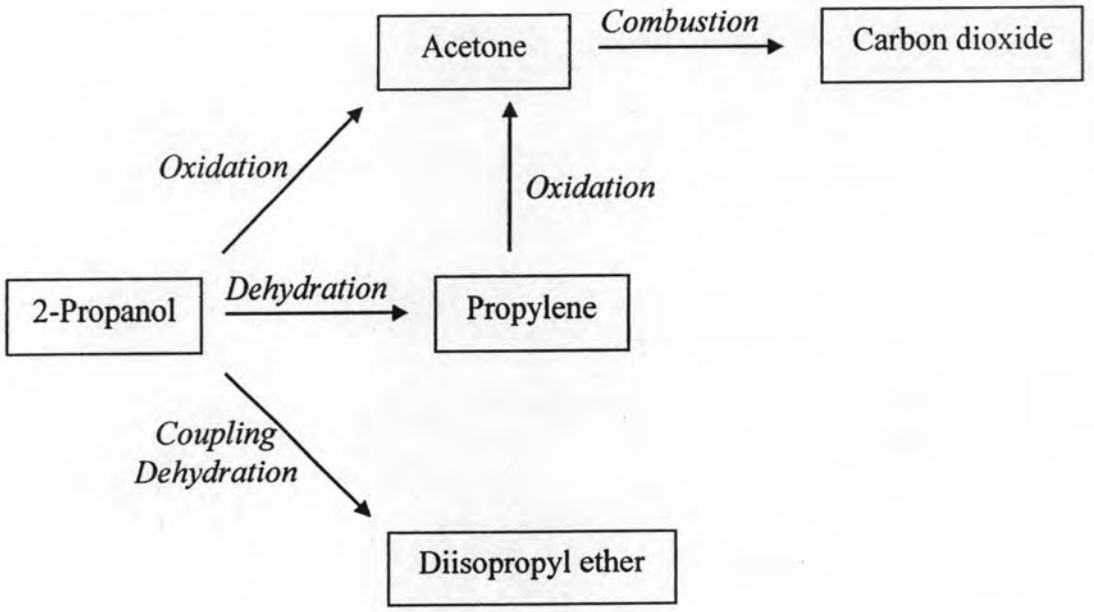

Figure 5.7 Schematic pathway of product formation in 2-propanol oxidation reaction.

The oxidation reaction from Figure 5.6 shows the poor grams mole of products below the reaction temperature of 250°C. At the higher reaction temperature, however the products rapidly increased in the reaction temperature range 300-400°C. Especially, acetone is the primary product with highest amount in the reaction while carbon dioxide became significant in the reaction temperature above 300°C. The other figures of grams

mole products which used different cobalt salts (nitrate, acetate, chloride) and various loading solutions (A1, A2, C1 and A1A2) are shown in Appendix E. These results showed the similar behavior like Figure 5.6 in distinct quantity of products at the same temperature. The conversion and product selectivities of 2-propanol as shown in Figures 5.8a-5.8j were selected to discuss the effect of parameters (cobalt salts and loading solutions) that used in Co-TS-1 catalyst preparation. The different cobalt salts (nitrate, chloride, acetate) in solutions have the same species of cobalt metal (Co^{2+}). Since the precipitation occurred, the cobalt species independent from cobalt salts. When catalyst is formed in the same species, the trendency of oxidation reaction has the similar behavior in all samples. Therefore, the distinct quantity of cobalt in framework which is the same species results in the different amount of products.

The effects of reaction temperature on the catalytic activity and product selectivities of 2-propanol over Co-TS-1 catalysts with different cobalt salts and loading solutions, are shown in Figures 5.8a-5.8j. It is found that all the synthesized Co-TS-1 samples behave in a similar way. The discrepancy between each catalyst is the amount of 2-propanol being converted to the products. The conversion of 2-propanol increased sharply in the reaction temperature range 300-450°C. The conversion rises up to about 93-95% conversion at about 500°C. As a result, the main products of this system are acetone, propylene and carbon dioxide. The amount of acetone was higher in the low reaction temperature range and decreased when temperature raised up while propylene and carbon dioxide gradually increase when temperature raised up. From previous result, carbon dioxide became significant in the reaction temperature above 300°C. It can be seen that the product of carbon dioxide relates to the lowering of acetone and propylene. Therefore, it can be concluded that the acetone and propylene were oxidized to combustion product, CO_2, at high temperature. The selectivities to carbon dioxide are around 20-30% in the reaction temperature range 450-500°C. From these results it can be concluded that acetone is the primary oxidation product (with selectivity almost 100% at 200°C), which is produced directly from the 2-propanol oxidation reactions. But the formation of the dehydration was not totally excluded. The less of propylene formation shows that the oxidation well occurs than the dehydration. The reduction of propylene formation in the high reaction temperature region is possibly because of the fast oxidation

of 2-propanol to acetone. Therefore, there was no enough 2-propanol to produced propylene. Another assumption is the oxidation of propylene to acetone.

The effect of incorporated cobalt metal into TS-1 framework with different parameters that used in preparation step was interpreted into three following sections, selective oxidation, dehydration ability and combustion ability.

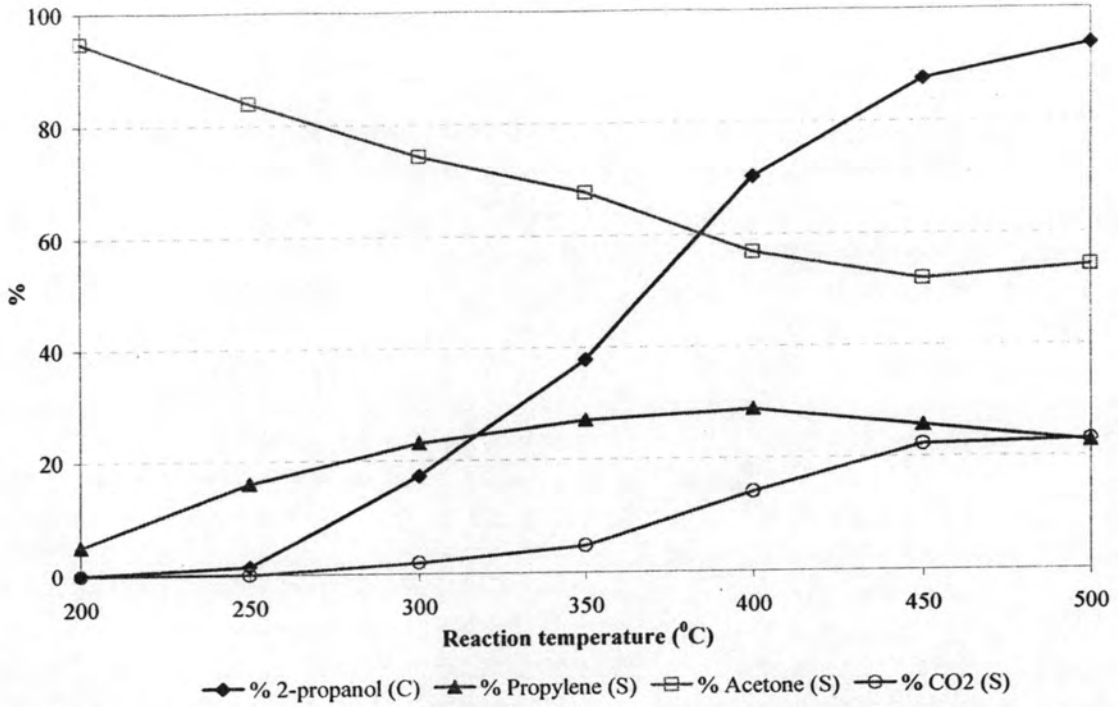

Figure 5.8a The conversion (C) and selectivity (S) of 2-propanol over Co-TS-1 for 8 Vol% O_2 system ($Co(NO_3)_2 \cdot 6H_2O$ loading to A1).

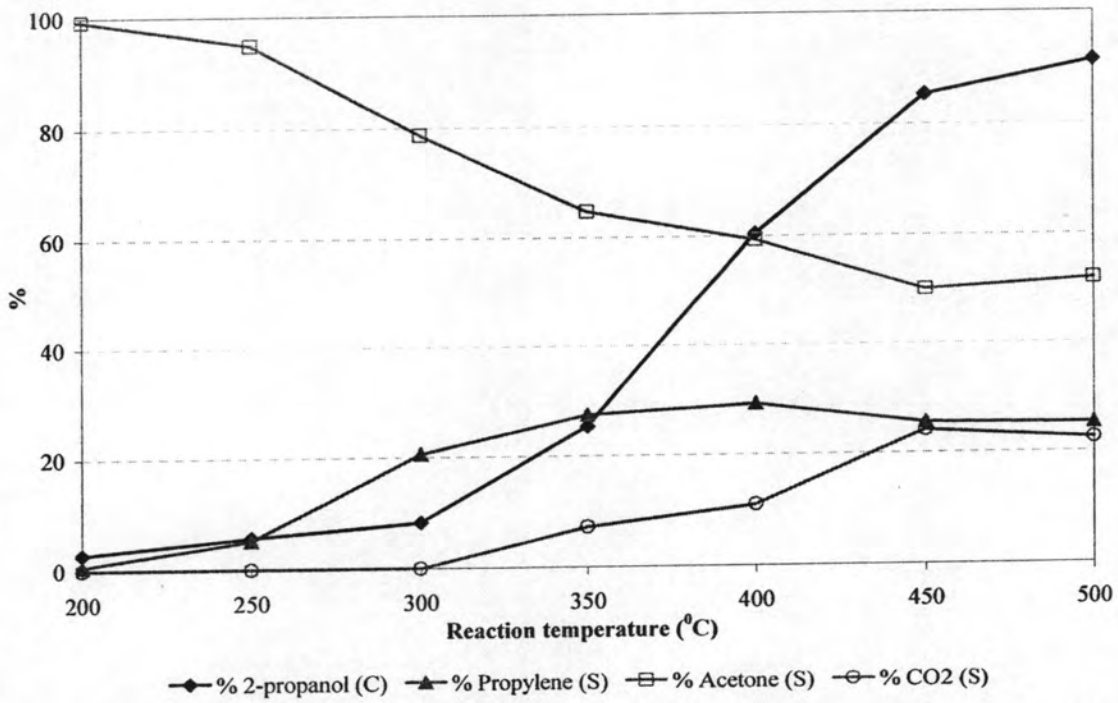

Figure 5.8b The conversion (C) and selectivity (S) of 2-propanol over Co-TS-1 for 8 Vol% O_2 system ($Co(NO_3)_2 \cdot 6H_2O$ loading to A2).

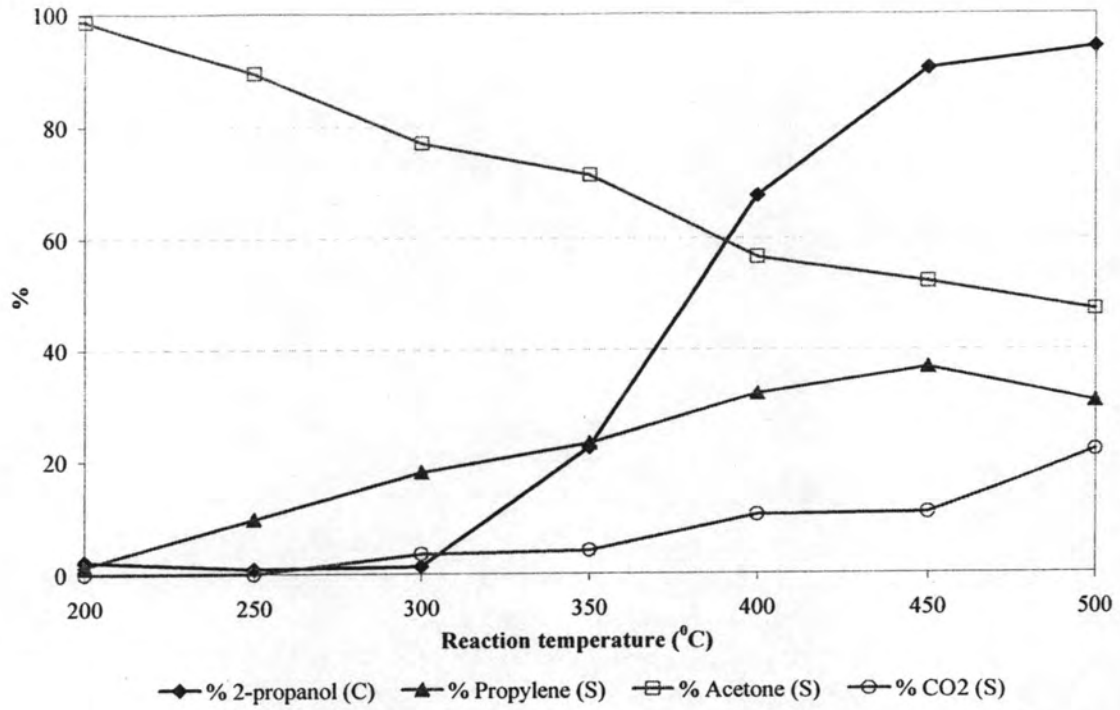

Figure 5.8c The conversion (C) and selectivity (S) of 2-propanol over Co-TS-1 for 8 Vol% O_2 system ($Co(NO_3)_2 \cdot 6H_2O$ loading to C1).

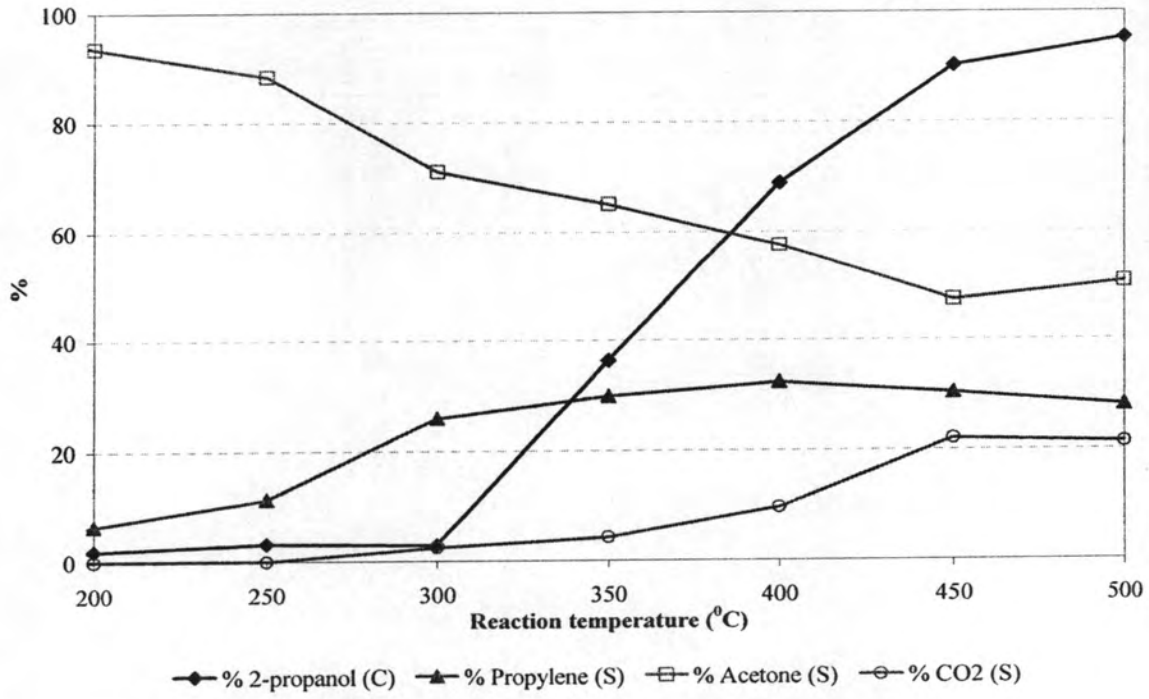

Figure 5.8d The conversion (C) and selectivity (S) of 2-propanol over Co-TS-1 for 8 Vol% O_2 system ($Co(NO_3)_2 \cdot 6H_2O$ loading to A1 and A2).

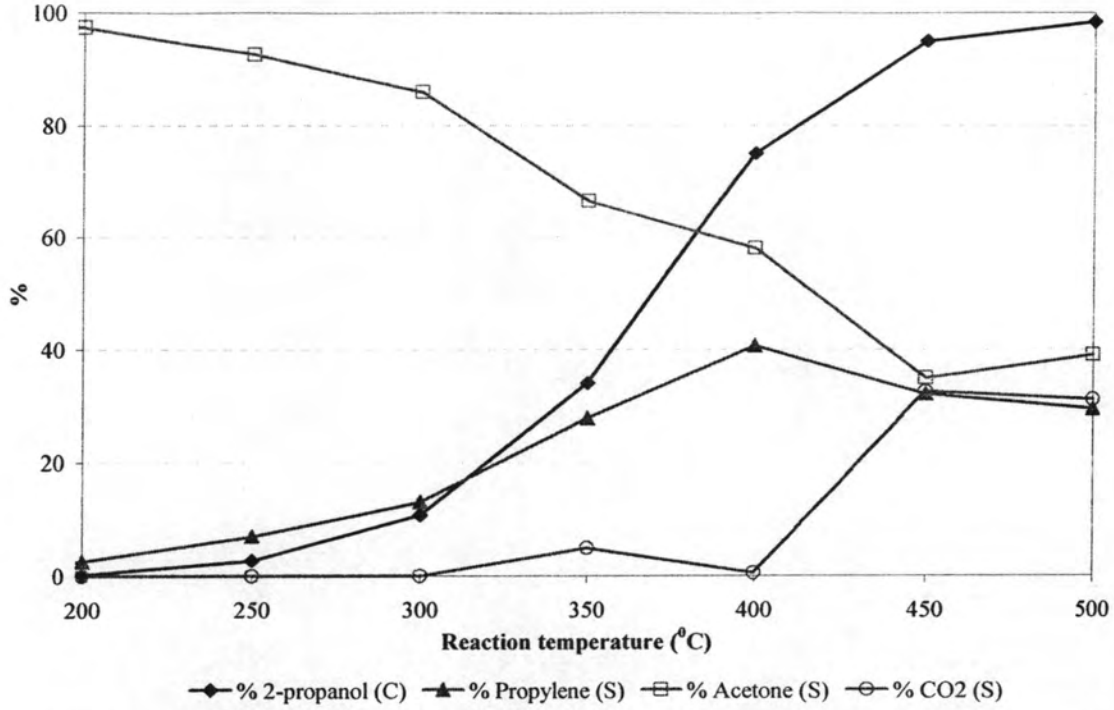

Figure 5.8e The conversion (C) and selectivity (S) of 2-propanol over Co-TS-1 for 8 Vol% O_2 system ($CoCl_2 \cdot 6H_2O$ loading to A1).

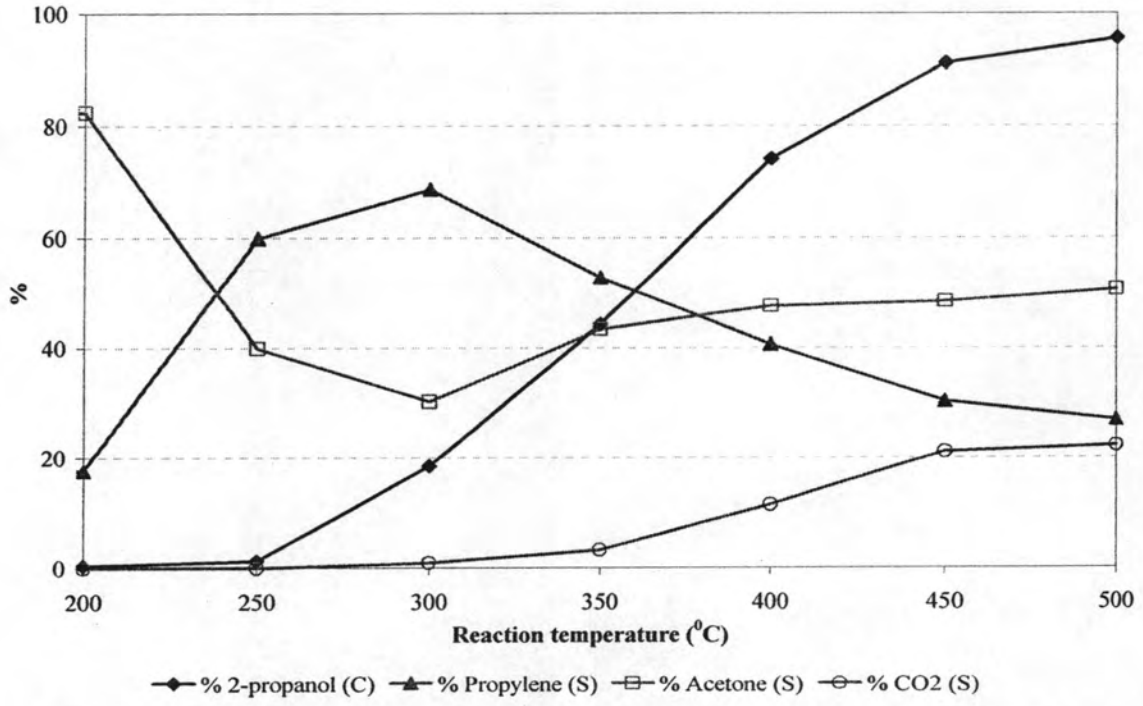

Figure 5.8f The conversion (C) and selectivity (S) of 2-propanol over Co-TS-1 for 8 Vol% O_2 system ($CoCl_2 \cdot 6H_2O$ loading to C1).

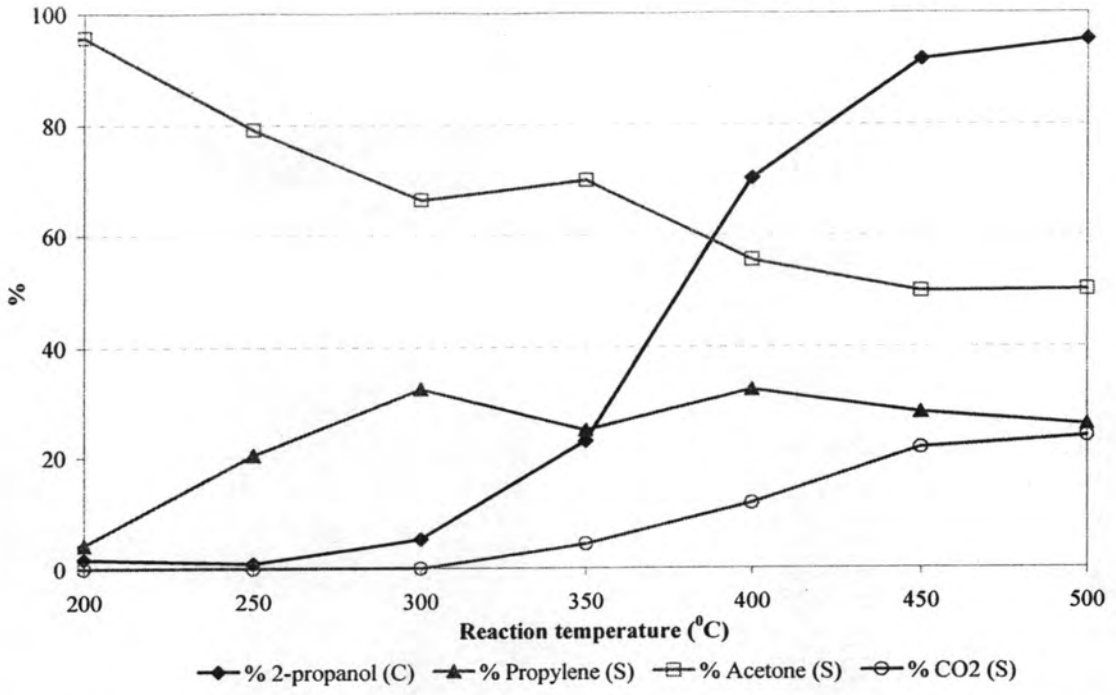

Figure 5.8g The conversion (C) and selectivity (S) of 2-propanol over Co-TS-1 for 8 Vol% O_2 system ($CoCl_2 \cdot 6H_2O$ loading to A1 and A2).

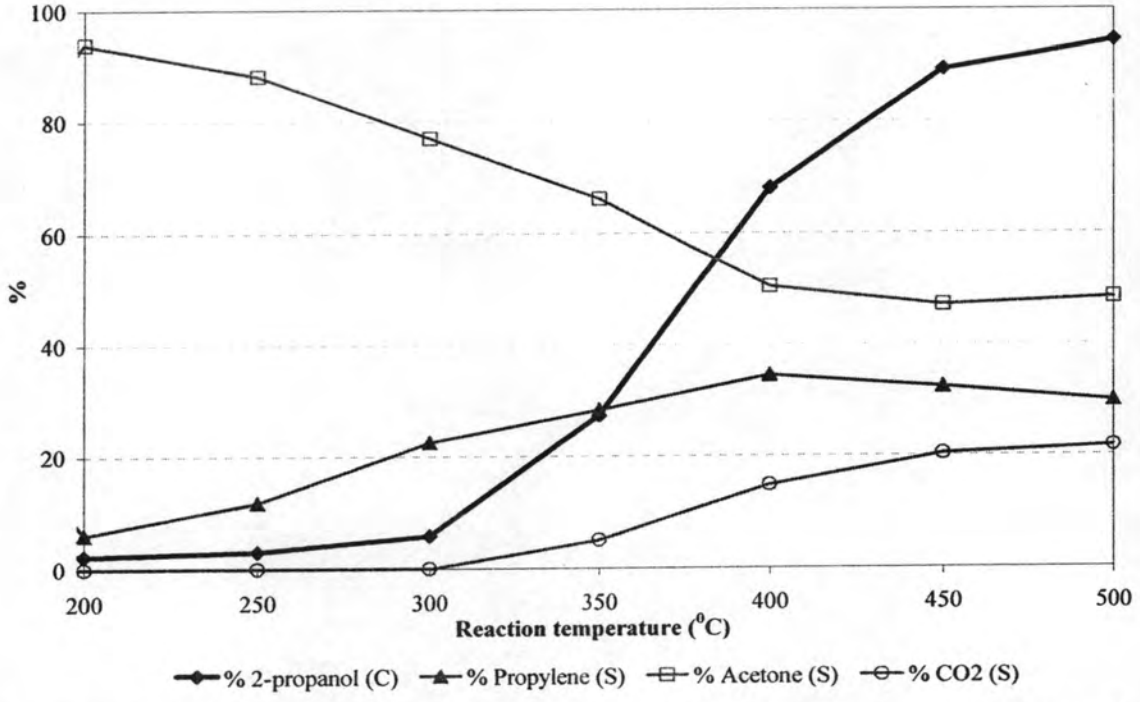

Figure 5.8h The conversion (C) and selectivity (S) of 2-propanol over Co-TS-1 for 8 Vol% O_2 system ($Co(C_2H_3O_2)_2 \cdot 4H_2O$ loading to A1).

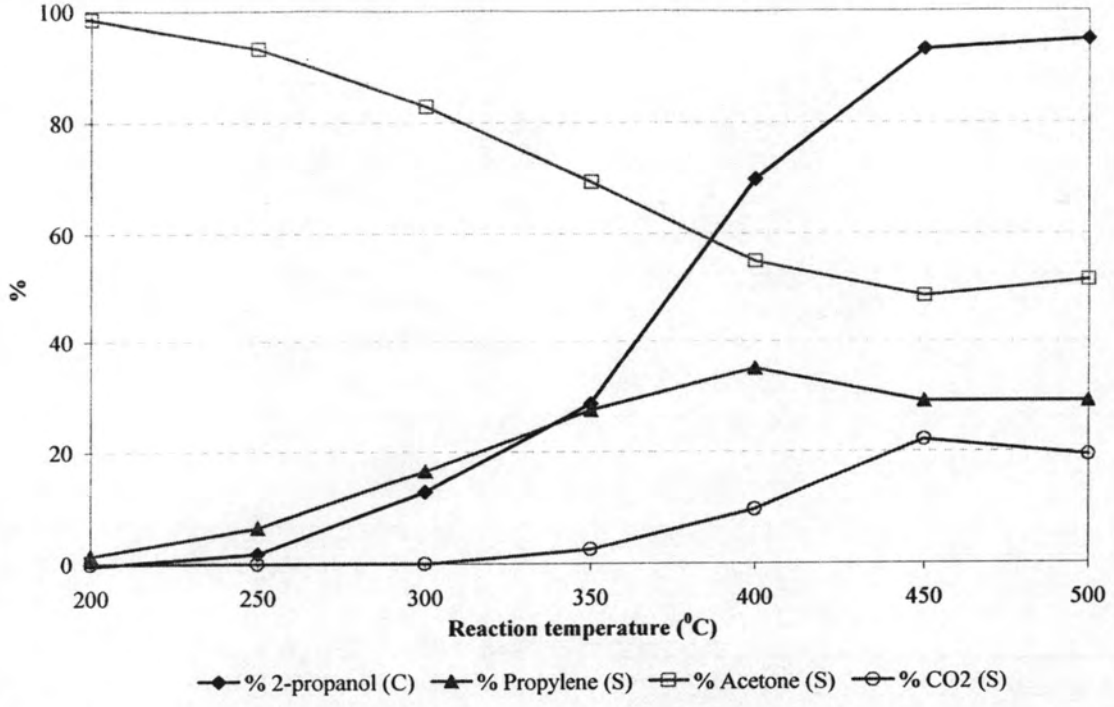

Figure 5.8i The conversion (C) and selectivity (S) of 2-propanol over Co-TS-1 for 8 Vol% O_2 system ($Co(C_2H_3O_2)_2 \cdot 4H_2O$ loading to C1).

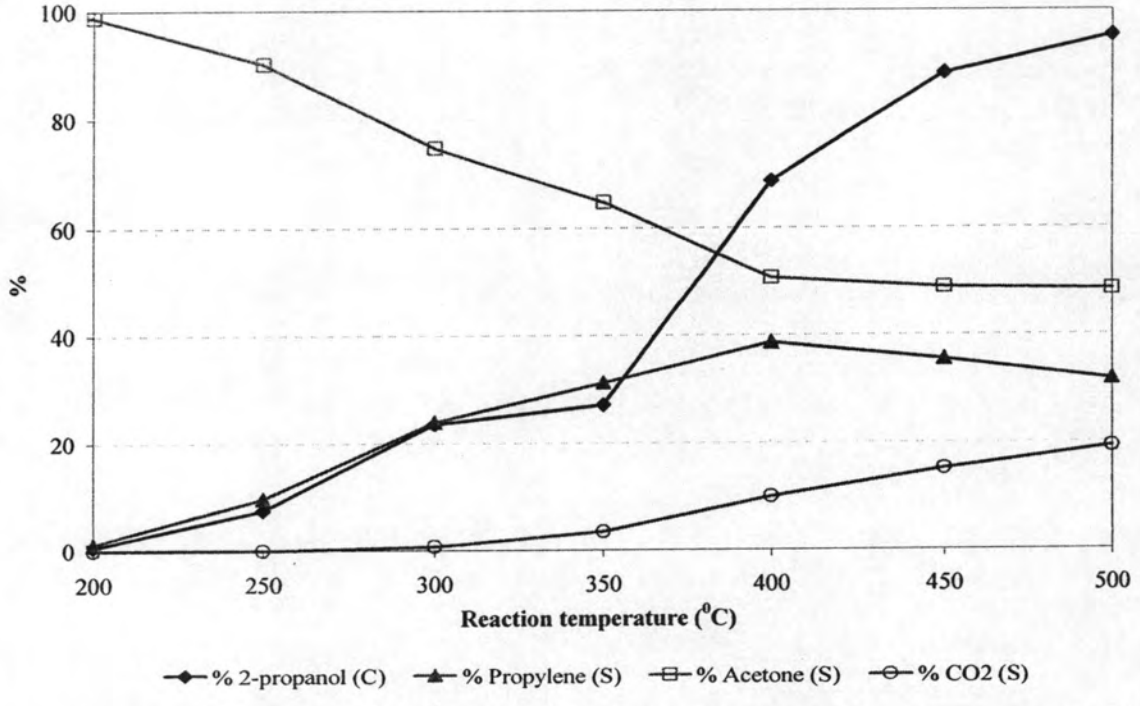

Figure 5.8j The conversion (C) and selectivity (S) of 2-propanol over Co-TS-1 for 8 Vol% O_2 system ($Co(C_2H_3O_2)_2 \cdot 4H_2O$ loading to A1 and A2).

5.2.1 Selective oxidation ability

Selective oxidation is a reaction which depends on oxygen. From Figures 5.8a-5.8j, we found that the trend of selectivities of all samples is almost the same. The changing in acetone selectivity can be the result of the further oxidation of acetone to CO_2 or the competitive reaction between the dehydration of 2-propanol to propylene and the oxidation of 2-propanol to acetone.

Comparison Co-TS-1 sample that used $Co(C_2H_3O_2)_2 \cdot 4H_2O$ as a cobalt salt between loading to C1 solution and A1 solution. Acetone selectivity of loaded cobalt into A1 solution is lower when compare with the loaded cobalt into C1 solution because of the lower amount of titanium for A1 solution. This comparison also confirms that Ti^{4+} exists in Co-TS-1 framework from the appearance of acetone.

From the results showed in Figures 5.8a-5.8j, the acetone selectivity will drop with decreasing of titanium in the synthesized Co-TS-1 samples except the samples of $Co(NO_3)_2 \cdot 6H_2O$ loading to A2 and A1A2 solutions which rarely have cobalt metal in framework. The reason may be the seldom cobalt metal in samples cause Ti^{4+} in silicate framework increased. By considering the increasing of titanium that can be incorporated into the framework, one would except non-framework titanium species to be formed. The non-framework titanium species might lead to the decomposition of active site for the selective oxidation. As a result, a lowering of the catalytic activity will be observed even though the amount of titanium increased. Hence, the catalytic activity of acetone depends on not only the amount of titanium in framework but also concern about non-framework titanium species.

In case of Co-TS-1 ($CoCl_2 \cdot 6H_2O$ loading to C1), acetone selectivity decreased sharply at the low temperature (<300°C) as seen in Figure 5.8f. Since the formation of CO_2 does not significantly change while the formation of propylene is significantly increased, the observed decrease of acetone selectivity is likely to be the result of loosing 2-propanol reactant to propylene rather than the loosing via the further oxidation of acetone to CO_2.

5.2.2 Dehydration ability

Dehydration is a reaction which produces the molecule of alkenes and water by the elimination of OH^- group and H atom that attached to carbon atom as described in chapter II. In case of dehydration of 2-propanol, propylene and water become our products. Dehydration reaction can progress without oxygen, but need suitable acidity. More quantities of acid sites, more dehydration can occur.

The dehydration reaction tests with Co-TS-1 samples are showed in Figures 5.8a-5.8j. From these results, the propylene selectivity increased slightly when temperature raised. Then, with a further increase of temperature, the catalytic activity decreased slightly. The maximum selectivities toward propylene are obtained at vary temperature by using the nitrate salt (28.71% in 400°C, 29.22% in 400°C, 36.83% in 450°C and 32.44% in 400°C for loading in A1, A2, C1 and A1A2 solutions, respectively), the chloride salt (40.69% in 400°C, 68.64% in 300°C and 32.38% in 400°C for loading in A1, C1 and A1A2 solutions, respectively) and the acetate salt (34.52% in 400°C, 35.04% in 400°C and 38.73% in 400°C for loading in A1, C1 and A1A2 solutions, respectively). This behavior indicates that propylene is the essential product likely be produced via the dehydration of 2-propanol as seen in Figure 5.7.

In each types of salts (nitrate, chloride, acetate) that used as cobalt source, the catalytic activity of dehydration is rather higher with increased amount of cobalt in Co-TS-1 samples, except the Co-TS-1 ($Co(NO_3)_2 \cdot 6H_2O$ loading to A1). By considering this unusual behavior, the high quantity of cobalt metal that incorporated into the framework might lead to conceal the Ti^{4+} active sites. As a result, a lowering of the catalytic activity will be observed. Moreover, the increased amount of cobalt in Co-TS-1 catalysts results in the raising of weaker acid sites which satisfy for dehydration reaction. Therefore, the high ratio of weaker acid sites corresponds to increase dehydration ability.

In order to confirm the effect of cobalt metal on the dehydration ability, comparative Co-TS-1 catalysts among batch 2, batch 5 and batch 7 (Figures 5.8b, 5.8e and 5.8g, respectively) which have equivalent titanium but differ in amount of cobalt. The results show that the increasing of cobalt metal promotes higher catalytic activity for

dehydration reaction rather than the selective oxidation. Furthermore, the CO_2 selectivity also increased with increasing amount of cobalt metal.

5.2.3 Combustion ability

Combustion is a complete oxidation reaction which also needs oxygen. From each figure in this part, we will see that CO_2 selectivity is increased simultaneous with decreasing of acetone and propylene selectivities. It can be interpreted that some parts of acetone and propylene are burned with oxygen. In addition, CO_2 selectivity will be limited at 40% because of the limited amount of oxygen in our system.

From Figure 5.8a-5.8j, we found that the raising of CO_2 selectivity became significant at temperature above 300°C. Even though, at the low temperature, the decreasing of acetone and propylene selectivities occurred, the CO_2 selectivity still disappeared. Hence, lowering the acetone and propylene does not lead to the appearance of CO_2 selectivity at the low temperature (<300°C). The abnormal behavior may occur out of the coking on catalyst which results from the combustion on catalyst with oxygen. In addition, the spent catalysts after reaction have obviously changed colour into black powder for every samples. Because of the accumulated carbon in catalyst at low temperature and exhaust at high temperature, the mass balance of input and output does not slightly equilibrate at the high temperature. To confirm this assumption, DSC-TGA analysis is chosen as demonstrated in Figure 5.9.

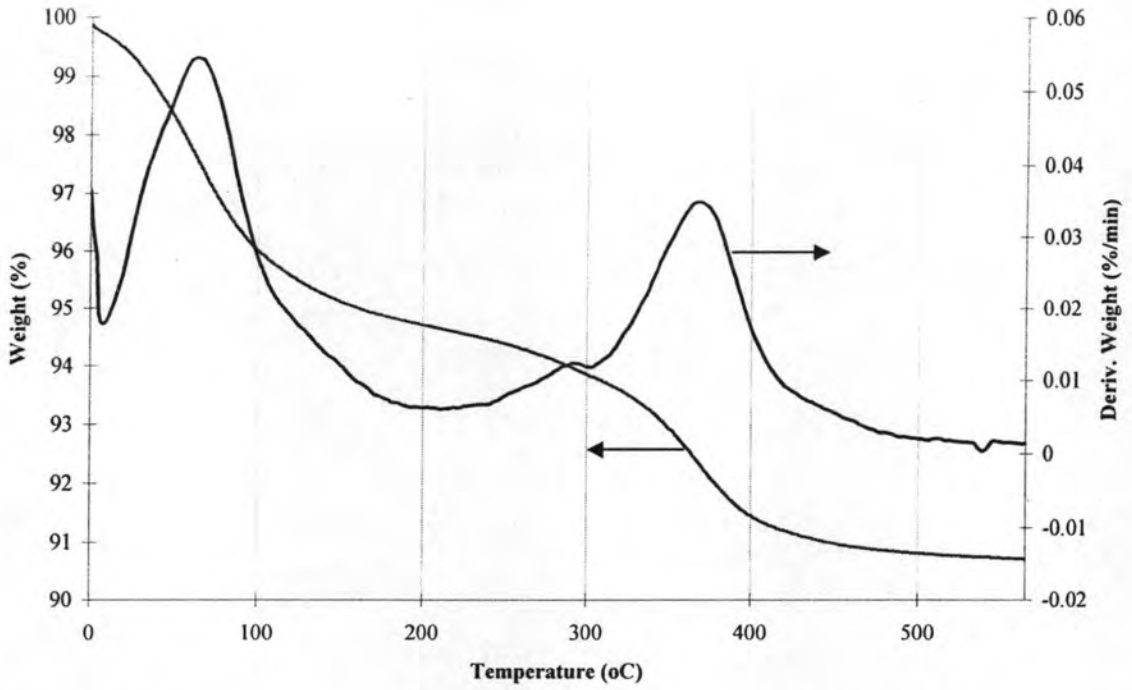

Figure 5.9 TGA analysis the spent Co-TS-1 ($CoCl_2 \cdot 6H_2O$ loading to C1) catalysts.

The TGA analysis of the spent Co-TS-1 ($CoCl_2 \cdot 6H_2O$ loading to C1) catalyst after reaction at 100-500°C present weight loss in two peaks centered, 100 and 400°C, with a proportion on 3-5 wt% and 4 wt%, respectively. The first peak at 100°C is the weight loss of water and another at 400°C is believed to be the weight loss of carbon. Since the maximum adsorption capacity of Co-TS-1 is about 9 wt%, this result suggests that the carbon is really present within the Co-TS-1 catalyst pores. It is known that the equilibrium of the adsorption phenomenon is favored at low temperature. This high concentration of products within the zeolite pores leads probably to important diffusion limitations, which may also affect negatively the catalytic activity compared to the fresh Co-TS-1 samples.

From our experiment, the combustion of acetone and propylene well occurs in reaction test with Co-TS-1 ($CoCl_2 \cdot 6H_2O$ loading to A1) catalyst that produced the maximum CO_2 selectivity at high temperature, as we see in Figure 5.8e. The raising of CO_2 selectivity coupled with high selectivity of acetone and propylene below 400°C. Therefore, the accumulation of carbon is exhausted in the high value at 400-500°C as shown in Figure 5.9.

Consequently, the ratio of weaker acid site on the catalyst surface is increased with more loaded cobalt in TS-1 framework for each cobalt salt. Moreover, we also known that high ratio of weaker acid site leads to increase dehydration ability except the sample which prepared by $Co(NO_3)_2 \cdot 6H_2O$ loading to A1. As a result, the highest selectivity of propylene from reaction test with loading to C1 solutions for all types of cobalt salt is the best condition. Another conclusion for selective oxidation, we found that the number of Ti^{4+} in the silicate framework correspond to increasing of acetone ability except the nitrate salt that loading to A2 and A1A2 solutions.